Finch, N. C., Fawaz, S., Neal, C. R., Butler, M. J., Salmon, A., Lay, A. C., Stevens, M., Mellor, H. H., Harper, S. J., Welsh, G. I., Foster, R., & Satchell, S. C. (2022). Reduced glomerular filtration in diabetes is attributable to loss of density and increased resistance of glomerular endothelial cell fenestrations. *Journal of the American Society of Nephrology*, *33*(6), 1120-1136. https://doi.org/10.1681/ASN.2021030294

JASN Journal of the American Society of Nephrology

Reduced Glomerular Filtration in Diabetes is Attributable to Loss of Density and Increased Resistance of Glomerular Endothelial Cell Fenestrations

Journal:	*Journal of the American Society of Nephrology*
Manuscript ID	JASN-2021-03-0294.R2
Manuscript Type:	Original Article - Basic Research
Date Submitted by the Author:	20-Dec-2021
Complete List of Authors:	Finch, Natalie; Bristol Medical School, Bristol Renal Fawaz, Sarah; Bristol Medical School, Bristol Renal Neal, Chris; Bristol Medical School, Bristol Renal Butler, Matthew; Bristol Medical School, Bristol Renal Lee, Vivian; University College London Institute of Ophthalmology, Translational Vision Research Salmon, Andrew; Waitemata District Health Board, Renal Service Lay, Abigail; Bristol Medical School, Bristol Renal Stevens, Megan; University of Exeter Medical School, Institute of Biomedical and Clinical Sciences Dalayan, Lusyan; Bristol Medical School, Bristol Renal Band, Hamid; University of Nebraska Medical Center Eppley Institute for Research in Cancer and Allied Diseases; University of Nebraska Medical Center Fred & Pamela Buffett Cancer Center Mellor, Harry; University of Bristol, School of Biochemistry Harper, Steven; Bristol Medical School, Bristol Renal Shima, David; University College London Institute of Ophthalmology, Translational Vision Research Welsh, Gavin; Bristol Medical School, Bristol Renal Foster, Rebecca; Bristol Medical School, Bristol Renal Satchell, Simon; Bristol Medical School, Bristol Renal
Keywords:	cell biology and structure, diabetic nephropathy, glomerular endothelial cells, glomerular filtration barrier, ultrafiltration, water permeability

Authors: Finch, Natalie; Fawaz, Sarah; Neal, Chris; Butler, Matthew; Lee, Vivian; Salmon, Andrew; Lay, Abigail; Stevens, Megan; Dalayan, Lusyan; Band, Hamid; Mellor, Harry; Harper, Steven; Shima, David; Welsh, Gavin; Foster, Rebecca; Satchell, Simon

Title: Reduced Glomerular Filtration in Diabetes is Attributable to Loss of Density and Increased Resistance of Glomerular Endothelial Cell Fenestrations

Running title: Glomerular endothelial fenestrae

Manuscript Type: Original Article - Basic Research

Manuscript Category: Other

Funders: Wellcome Trust, (Grant / Award Number: '104507/Z/14/Z')

Financial Disclosure: No N. Finch reports Research Funding: Boehringer Animal Health; and Scientific Advisor or Membership: Governing Council of the Cat Fancy. A. Salmon reports Advisory or Leadership Role: Kidney Health New Zealand. H. Band reports Patents and Inventions: EMD-Millipore, Amgen (one time), and Genentech (one time). S. Harper reports Consultancy: Exonate Ltd; Ownership Interest: Exonate Ltd, Emenda Therapeutics Ltd, Four Rivers Renal Services Ltd, Patents or Royalties: Via University of Bristol revenue sharing; and Advisory or Leadership Role: Exonate Ltd Board Member & Co-Founder, Emenda Therapeutics Board Member & Co-Founder, Four Rivers Renal Services Board Member and Founder. D. Shima reports Scientific Advisor or Membership: American Journal of Pathology Editorial Board G. Welsh reports Consultancy Agreements: Purespring Therapeutics; and Research Funding: Travere Therapeutics. S. Satchell reports Consultancy Agreements: Novo Nordisk, Research Funding: Ferring, Evotec, Novo Nordisk; Scientific Advisor or Membership: Kidney Research UK Grants Committee; and Other Interests/Relationships: Member of the UK Kidney Association.

Study Group/Organization Name: CUST_STUDY_GROUP/ORGANIZATION_NAME :No data available.

Study Group Members' Names: CUST_STUDY_GROUP_MEMBERS :No data available.

Total number of words: 3754

Abstract: Background: Glomerular endothelial cell (GEnC) fenestrations are recognised as an essential component of the glomerular filtration barrier, yet little is known about how they are regulated and their role in disease.
Methods: We comprehensively characterized GEnC fenestral and functional renal filtration changes including measurement of glomerular ultrafiltration coefficient and glomerular filtration rate in diabetic mice (BTBR ob⁻/ob⁻). We also examined and compared human samples. We evaluated Eps homology domain protein-3 (EHD3) and its association with GEnC fenestrations in diabetes in disease samples and further explore its role as a potential regulator of fenestrations in an in vitro model of fenestration formation using b.End5 cells.
Results: Loss of GEnC fenestration density was associated with decreased filtration function in diabetic nephropathy. We identified increased diaphragmed fenestrations in diabetes, which are posited to increase resistance to filtration and further contribute to decreased GFR. We identified decreased glomerular EHD3 expression in diabetes, which was significantly correlated with decreased fenestration

density. Reduced fenestrations in EHD3 knock-down b.End5 cells in vitro further suggested a mechanistic role for EHD3 in fenestration formation.
Conclusions: This study demonstrates the critical role of GEnC fenestrations in renal filtration function and suggests EHD3 may be a key regulator, loss of which may contribute to declining glomerular filtration function through aberrant GEnC fenestration regulation. This points to EHD3 as a novel therapeutic target to restore filtration function in disease

Significance Statement

We propose a novel mechanism underlying loss of renal filtration function from studying glomerular endothelial cell (GEnC) fenestrae in human diabetic kidney tissue and in a mouse model of diabetes. Diaphragmed fenestrae may provide structural resistance to filtration. We hypothesize that EHD3 is a key regulator of GEnC fenestrations, and its glomerular expression is lost in diabetes. This study establishes the critical role of GEnC fenestrations in renal filtration function and suggests a key regulator, potentially paving the way for development of targeted therapies to restore fenestrae and thus filtration function in kidney disease.

Reduced Glomerular Filtration in Diabetes is Attributable to Loss of Density and Increased Resistance of Glomerular Endothelial Cell Fenestrations

Natalie C Finch†, Sarah S Fawaz†, Chris R Neal†, Mathew J Butler†, Vivian K Lee††, Andrew J Salmon†††, Abigail C Lay†, Megan Stevens††††, Lusyan Dayalan†, Hamid Band†††††, Harry H Mellor††††††, Steven J Harper†, David T Shima††, Gavin I Welsh†, Rebecca R Foster†, Simon C Satchell†.

† Bristol Renal, Bristol Medical School, University of Bristol, Bristol

†† Translational Vision Research, Institute of Ophthalmology, University College London, London

††† Renal Service, Waitemata DHB, Auckland, New Zealand

†††† Institute of Biomedical and Clinical Sciences, University of Exeter Medical School, Exeter

††††† Eppley Institute for Research in Cancer, and Fred & Pamela Buffett Cancer Center, University of Nebraska Medical Center, Omaha, NE, USA.

†††††† School of Biochemistry, University of Bristol, Bristol

Short running title: Glomerular endothelial fenestrae

Word count (abstract): 227
Word count (introduction, results and discussion): 3403

Corresponding author: Natalie C Finch, Bristol Renal, Bristol Medical School, University of Bristol, Dorothy Hodgkin Building, Whitson Street, Bristol, UK, BS1 3NY, natalie.finch@bristol.ac.uk

Key words: Glomerular endothelial cell fenestrations, glomerular ultrafiltration coefficient, glomerular filtration rate, diabetes, Ehd3

Abstract

Background: Glomerular endothelial cell (GEnC) fenestrations are recognised as an essential component of the glomerular filtration barrier, yet little is known about how they are regulated and their role in disease.

Methods: We comprehensively characterized GEnC fenestral and functional renal filtration changes including measurement of glomerular ultrafiltration coefficient and glomerular filtration rate in diabetic mice (BTBR *ob*$^{-}$/*ob*$^{-}$). We also examined and compared human samples. We evaluated Eps homology domain protein-3 (EHD3) and its association with GEnC fenestrations in diabetes in disease samples and further explore its role as a potential regulator of fenestrations in an *in vitro* model of fenestration formation using b.End5 cells.

Results: Loss of GEnC fenestration density was associated with decreased filtration function in diabetic nephropathy. We identified increased diaphragmed fenestrations in diabetes, which are posited to increase resistance to filtration and further contribute to decreased GFR. We identified decreased glomerular EHD3 expression in diabetes, which was significantly correlated with decreased fenestration density. Reduced fenestrations in EHD3 knock-down b.End5 cells *in vitro* further suggested a mechanistic role for EHD3 in fenestration formation.

Conclusions: This study demonstrates the critical role of GEnC fenestrations in renal filtration function and suggests EHD3 may be a key regulator, loss of which may contribute to declining glomerular filtration function through aberrant GEnC fenestration regulation. This points to EHD3 as a novel therapeutic target to restore filtration function in disease.

Introduction

Glomerular endothelial cells (GEnC) are highly differentiated endothelial cells lining the glomerular capillaries. They are perforated with transcellular pores, reportedly 60-80nm in diameter, known as fenestrations.[1] GEnC fenestrations allow the passage of fluid and small solutes from the glomerular capillary lumen through the endothelial cells, without the need for endocytosis or receptor-mediated mechanisms. GEnC fenestrations are transcellular pores containing glycocalyx proteoglycans and glycoproteins. Unlike most fenestrated endothelia, mature, fully differentiated quiescent GEnC have predominantly non-diaphragmed fenestrations,[1] enabling high fluid flux driven by hydrostatic pressure. In addition, they do not express the fenestral/caveolar diaphragm protein PVLAP. Alterations in GEnC fenestration density or diameter pose an important potential mechanism for regulating glomerular filtration and may play a critical role in pathogenesis of diseases characterised by a decline in glomerular filtration rate (GFR).

The glomerular ultrafiltration coefficient (L_PA/Vi) can be determined in isolated glomeruli using an oncometric assay.[2-5] This allows the evaluation of hydraulic permeability of the glomerular filtration barrier in isolation from circulating and haemodynamic factors. Measurement of L_PA/Vi allows the relationship between ultrastructural components of the glomerular filtration barrier and filtration function to be evaluated. Relationships between GEnC fenestrations and L_PA/Vi are poorly described. Some mathematical models suggest that the glomerular endothelium provides little resistance to hydraulic permeability.[6] However, it has been

observed that decreased GEnC fenestration density is associated with decreased hydraulic permeability in women with pre-eclampsia.[7] Furthermore, decreased L_PA/Vi has been demonstrated in $VEGF_{165}b$ overexpressing mice with decreased GEnC fenestration density.[5] Relationships between GEnC fenestrations and direct measurements of L_PA/Vi, and GFR have not previously been described.

Diabetic nephropathy is the leading cause of end stage renal disease. It is characterised by glomerular hypertrophy and hyperfiltration in early disease and progressive albuminuria, decline in GFR and glomerular and tubulointerstitial structural changes in late disease.[8] Loss of GEnC fenestrations is observed in advanced diabetic nephropathy alongside reduced GFR.[9] Decreased percentage of fenestrated endothelium is correlated with decreased GFR in people with type 2 diabetes[9, 10] and also reported in people with type 1 diabetes.[11] BTBR *ob*$^{-}$/*ob*$^{-}$ mice develop type 2 diabetes and progressive diabetic nephropathy.[12] Their susceptibility to diabetic nephropathy has been suggested to be related to endothelial dysfunction, similar to that seen in eNOS-deficient mice.[12] However, GEnC fenestral ultrastructural changes in this model have not been described.

Eps15 homology domain-containing proteins 3 and 4 (EHD3 and 4) are endosomal transport proteins.[13] Within the kidney, EHD3 is specifically expressed in GEnC[14, 15] and has been localised to the fenestrae.[14] Single cell transcriptome profiling also demonstrates that within the glomerulus, EHD3 expression is high in the fenestrated capillary endothelial cells compared to

the non-fenestrated arteriolar (afferent and efferent) cells.[16] EHD4 is highly expressed in peritubular capillary endothelial cells with very low expression in GEnC under normal conditions.[17] Dual knockout of Ehd3 (the murine nomenclature) and 4 in mice resulted in development of lesions consistent with thrombotic microangiopathy and absence of GEnC fenestrations.[17] Fenestral ultrastructural changes were not evaluated. However, the findings suggest a critical role for EHD3 in GEnC including as a candidate regulator of GEnC fenestrations.

In this study, we examine the role of GEnC fenestrations in glomerular filtration in diabetes, in both the BTBR *ob*$^{-}$*/ob*$^{-}$ mouse model and patient samples. We also examine glomerular EHD3 expression in diabetes and its role in fenestration regulation. We hypothesize that: (1) ultrastructural changes in GEnC fenestrae develop in diabetes and contribute to impairment of renal filtration function; (2) glomerular EHD3 expression decreases in diabetes alongside changes in GEnC fenestration measurements and GFR; (3) *in vitro* loss of EHD3 results in decreased fenestration formation.

Methods

Mice

Male wild type (+/+) and homozygous BTBR *ob*$^{-}$*/ob*$^{-}$ mice were obtained from the Jackson laboratory (BTBR.Cg-*Lep*^{ob}/WiscJ; Bar Harbor, ME, USA). The mice were provided with food and

water *ad libitum* and maintained in a clean temperature-controlled environment under a 12-hour light/dark cycle. Animal experiments were conducted with approval by the UK Home Office and in accordance with the Animals (Scientific Procedures) Act 1986. Weekly measurement of body weight and bi-weekly blood glucose measurement via tail vein blood collection was performed. At 20 weeks of age, mice underwent terminal anaesthesia via intraperitoneal injection of pentobarbitone (Euthatal 200mg/ml) and both kidneys were harvested and immediately processed as described in the following methods.

Renal functional measurements

Urinary albumin to creatinine ratio

Spot urine samples were collected bi-weekly. Mice were placed in a metabolic cage for up to 2 hours. Terminal urinary collection was performed via cystocentesis. Urinary albumin concentration was quantified using a mouse albumin ELISA (Bethyl Laboratories Inc; Montgomery, TX) and urinary creatinine concentration determined at a commercial reference laboratory (Langford Vets Diagnostic Laboratories, Bristol, UK) using an enzymatic spectrophotometric assay (Konelab T-Series 9812845; Thermo Fisher Scientific, Vantaa, Finland). Urinary albumin to creatinine ratio (uACR) was calculated as urinary albumin concentration/ urinary creatinine concentration.

Glomerular ultrafiltration coefficient (L_PA/V_i)

Glomeruli were isolated from freshly harvested kidney tissue using a standard sieving technique. L_PA was determined in individual glomeruli *ex vivo* within 4 hours of isolation, using a previously described oncometric method, and normalised to glomerular volume (L_PA/V_i).[2-5] Briefly, individual glomeruli were captured onto the tip of a suction micropipette within a flow controlled closed system. An oncotic pressure gradient was established across the glomerular capillary wall by exchanging the solution bathing the glomerulus from 10 $mg.ml^{-1}$ BSA to 80 $mg.ml^{-1}$. The resulting absorptive force draws fluid out of the glomerulus, resulting in a reduction in glomerular volume. The rate of glomerular volume change represents the rate at which fluid moves across the glomerular filtration barrier (J_V). Glomerular volume measurements were made from individual video images immediately before and after exchange of bathing solution. Glomerular L_pA ($nl.min^{-1}.mmHg^{-1}$) was calculated from the rate of glomerular volume change and applied oncotic pressure, as shown in the equation below:

$$L_pA = J_V/-\Delta\pi$$

Between 3 and 12 glomeruli per mouse were analysed using image analysis software (FIJI) by a blinded investigator.

Glomerular filtration rate

Glomerular filtration rate (GFR) was determined by measuring endogenous creatinine clearance. Within 24 hours of terminal anaesthesia mice were placed in a metabolic cage and timed urine collection performed over approximately six hours with exact time recorded in minutes. Plasma creatinine concentration was measured in a terminal blood collection sample collected into a heparinised plasma tube. Plasma and urinary creatinine concentration were

determined as described above. Endogenous creatinine clearance was calculated using the standard equation GFR (mL/min) = (U_{Cr} x V)/ (P_{Cr} x T) where U_{Cr} is urinary creatinine concentration (µmol/L), V is volume (mL), P_{Cr} is plasma creatinine concentration (µmol/L) and T is time (mins).

Transmission electron microscopy (TEM) to determine glomerular ultrastructural measurements

Immediately following terminal anaesthesia, kidney tissue was harvested and 1mm^3 diced kidney cortex obtained and transferred to 2.5% glutaraldehyde in 0.1 M cacodylate buffer. Samples were post-fixed in 1% osmium tetroxide, en bloc stained with uranyl acetate followed by ethanol dehydration and embedding in TAAB 812 resin (Agar Scientific). Sections were cut at 50-100nm using an ultramicrotome and stained with 3% aqueous uranyl acetate followed by Reynolds' lead citrate. Electron micrographs were acquired using a Technai 12 electron microscope (Thermofisher, UK). Additional kidney tissue from BTBR *ob/ob* mice aged 6, 10 and 15 weeks was contributed by University College London (DS) in 2.5% glutaraldehyde in 0.1 M cacodylate buffer and stored and shipped at 4^{o}C. Samples were processed as described above. Image analysis was performed by a blinded investigator using image analysis software (FIJI). Samples were chosen randomly as the orientation of each glomerulus in the section plane is unknown. Image acquisition was performed in a standardised manner by acquiring images from 3 glomeruli /mouse. Imaging areas were selected at the 12 and 6 o'clock position or at the 9 and 3 o'clock position if vascular poles or section folds intervened, derived from the low power

whole glomerulus image. A minimum of 6 images obtained at high magnification per glomeruli were analysed. Tangential and oblique cuts were ignored, and the presence of a phospholipid bilayer was taken as indicating that the endothelial and the podocyte membranes were aligned with the electron beam and therefore the section plane perpendicular to it. The unfenestrated GEnC body was not included in the image analysis. GEnC fenestration density was determined by counting the number of fenestrations per unit length of the GEnC peripheral cytoplasm. Glomerular endothelial cell fenestration width was determined by measuring the diameter of the fenestration at the narrowest distance between the opposing cell membranes. Diaphragms were identified as a single clear line of electron dense material spanning the fenestration and determined as the percentage of the total number of fenestrations. GEnC fenestration surface area was calculated as a percentage of measured GEnC surface area covered by total fenestration widths. Mean total length of endothelium analysed per mouse was 51542nm. Data regarding the total length of endothelium analysed is presented in supplementary information (S1). In addition, podocyte slit density, slit width, foot process width and glomerular basement membrane (GBM) thickness were determined. Mean values per individual were used for statistical analysis. Mathematical modelling to determine the contribution that the glomerular endothelium changes in diabetes make to the observed changes in functional properties of the glomerular capillary wall was performed using the approach described by Drumond & Deen[6] based on a unit cell of the glomerular capillary wall (See supplementary information S2).

PLVAP immunofluorescence to determine glomerular expression

Freshly harvested renal cortical tissue was immediately transferred to liquid nitrogen and stored at -80^{o}C. Frozen sections (4µm) of cortical tissue were cut at the University of Bristol Histology Service. Sections were briefly fixed in 4% (wt/vol) PFA followed by a blocking step (1% BSA in PBS). Primary antibody (Table 1) was applied to sections overnight. The following day sections were incubated with secondary antibody (1:200 anti-rat 488 Alexa Fluor, Life Technologies, Thermo Fisher Scientific) and the nuclei were counterstained with 4',6-diamidino-2-phenylindole (Invitrogen, Thermo Fisher Scientific). Sections were mounted in Vectashield mounting medium (Vector Laboratories). Image analysis was performed using an image software program (FIJI) by a blinded investigator. Corrected total glomerular fluorescence intensity was determined in three glomeruli per mouse and the mean for each mouse used in statistical analyses. Images were obtained at x40 magnification using an AF600 LX wide-field fluorescence microscope (Leica Microsystems, Milton Keynes, UK).

Ehd 3 and 4 immunohistochemistry to determine glomerular expression profiles

Freshly harvested cortical renal tissue was transferred to 4% (wt/vol) paraformaldehyde (PFA) for 48hrs hours. Dehydration and paraffin embedding were performed at the University of Bristol Histology Service. Sections (4µm) were cut using a microtome and transferred to glass slides. Deparaffinisation and hydration steps involved incubation in Histoclear II and decreasing concentrations of ethanol. Antigen retrieval was performed by heating sections in 10mM sodium citrate buffer (pH 6). Non-specific IgG binding was blocked with 1% BSA and 10% normal goat serum in TBS-Triton-X (0.1%). Primary antibodies (Table 1) or an IgG control were

applied to sections overnight. The following day endogenous peroxidase activity was blocked with 3% (wt/vol) hydrogen peroxide and sections incubated with an HRP conjugated secondary antibody specific for the antibody (SignalStain Boost IHC Detection Reagent, Cell Signaling, Danvers, MA, USA). Sections were subsequently incubated with DAB substrate (SignalStain DAB substrate, Cell Signaling, Danvers, MA, USA) and counter-stained with haematoxylin. Image analysis was performed using an image software program (FIJI) by a blinded investigator. Corrected total staining intensity was determined in three capillaries per glomeruli and three glomeruli per mouse and the mean for each mouse used in statistical analyses. Images were obtained at x40 magnification using light microscopy.

RNA extraction and qPCR to determine glomerular PLVAP, Ehd3 and Ehd4 mRNA expression.

Freshly sieved glomeruli were obtained from renal cortical sections by passing tissue through sequential sieves to extract the glomeruli and were immediately transferred to storage at -80°C prior to RNA extraction. Glomerular RNA extraction was performed using the Qiagen RNEasy kit (cat. no. 74104). Glomeruli were drawn repeatedly into a 0.5ml syringe to aid in cellular lysis. Following lysis, measurements of RNA concentrations were obtained using a nanophotometer (Pearl Implen, München, Germany) prior to cDNA conversion. RNA was converted to cDNA using a high capacity RNA-to-cDNA kit (ref 4387406; Applied Biosystems, Foster City, California, USA). The primers were designed using Eurofins; PLVAP Forward 5' CTATCATCCTGAGCGAGAAGC 3', Reverse 5' GCAGCAGGGTTGACTACAGG 3'; Ehd3 Forward 5'

CGCCGTGCTTGAAAGTATCAG 3', Reverse 5' ATAATTCGGTCCACCCGCTC 3'; Ehd4 Forward 5' ACCAAGTTCCACTCACTGAA 3', Reverse 5' GTTCATCTCCTCCTGGCTGA 3'. Optimum primer concentrations were established, and a standard protocol used for quantitative polymerase chain reaction (qPCR) analysis using the Fast Sybr Green master mix (ref 438612; Applied Biosystems). Statistical analyses were performed on delta cycle threshold values and data are shown as fold-change + SD.

Human samples

All studies on human kidney tissue were approved by national and local research ethics committees (REC) and conducted in accordance with the tenets of the Declaration of Helsinki. Transmission electron microscopy images and renal biopsy samples were obtained from Bristol, UK (Histopathology Department, Southmead Hospital) and were archived anonymously (REC H0102/45). Tissue was immersion fixed in 10% neutral buffered formalin and embedded in paraffin. Samples had been clinicopathologically diagnosed and included patients with diabetic nephropathy and patients with thin basement membrane or collagen 4 defect nephropathy which served as a control population. Patient eGFR, where available, was also provided. Transmission electron micrograph image analysis was performed as described above. In addition, kidney transplant tissue was also obtained and included in the control population for immunohistochemistry studies. Immunohistochemistry was performed as described above. Gene expression data were extracted from the Nephroseq database (www.nephroseq.org).

In vitro fenestration formation

A mouse brain endothelioma cell line (b.End5) was obtained from Culture Collections, Public Health England, Porton Down, UK) and maintained in high glucose DMEM (Sigma-Aldrich, Gillingham, UK) containing 10% FBS. An Ehd3 knockdown and control scrambled b.End5 cell line were generated. The lentiviral vectors containing mouse Ehd3 shRNA or scrambled sequences were purchased from Dharmacon Horizon Inspired cell solutions (VGH5526-EG57440). b.End5 at 40-60% confluency was incubated with the lentiviral particle in the presence of polybrene at 1:100 ratio for 4h in serum free media. The infected cells were cultured in complete media for 48h, followed by a puromycin selection at 0.8µg/ml for 3 consecutive days to obtain stable knockdown cell lines. The knockdown efficiency was confirmed by qPCR and Western blotting. Briefly, RNA was extracted from b.End5 cells (scrambled and knockdown) and PCR performed using the protocol described above. For Western blot analysis, b.End5 cells (scrambled and knockdown) were washed with PBS prior to protein extraction. The cells were lysed with ice-cold RIPA buffer (ThermoFisher Scientific # 89900) followed by centrifugation of lysates at 13000 rpm for 15 min at 4°C and collection of supernatants. Supernatant was added to Laemmli sample buffer at a 1:4 sample volume ratio, denatured in a heat block at 90°C for 10 minutes, separated on a 10% SDS-polyacrylamide gel and transferred to a polyvinylidene difluoride membrane. Following a blocking step (3% BSA prepared in Tris-buffered saline-tween (TBST; 20 nM Tris (pH 7.2), 150 mM NaCl, 0.1% Tween 20) for 1h, immunoblots were incubated overnight at 4 °C with primary antibodies to detect Ehd3 (Table 1). Housekeeping gene β-actin (1:5000; Millipore, Billerica, MA, USA) was used for normalization. Blots were incubated with secondary antibody for 1h at room temperature. Luminal and Femto peroxidase (Western ECL Substrate,

Biorad Clarity) were added in equal volumes (500µl each) to the membrane and the signal analysed using an Amersham imager 600 system. Densitometry was performed using ImageJ 1.43m software.

b.End5 cells were seeded at a density equivalent to 1.5 x 10^6 cells per 100mm dish[18, 19] onto gold grids on glass coverslips coated with pioloform. After 24hrs, fenestrations were induced with 1.25µM Latrunculin A (Sigma-Aldrich, Gillingham, UK) for 3hrs or 100ng/ml mouse $VEGF_{164}$ (R&D Systems, Minneapolis, USA) for 24hrs.[18, 19] Cells were fixed in 2.5% glutaraldehyde in 0.1 M cacodylate buffer, post-fixed in 1% osmium tetroxide followed by ethanol dehydration and dried using critical point drying. Wholemount cell samples were imaged using a Technai 12 electron microscope (FEI, Hillsboro, Oregan). Between 8 and 9 cells per treatment group were analysed. Fenestration density was determined in a 720nm^2 area in sieve plates in two separate sieve plate areas per cell. Fenestration width was measured for each individual fenestration in a 720nm^2 area. Mean fenestration density and width per cell was used for statistical analyses.

Statistical analyses

Statistical analysis was performed using GraphPad Prism (version 8, La Jolla, CA, USA). Gaussian distribution was demonstrated, and parametric statistical testing performed. Data are expressed as mean ± standard deviation (SD). Mean values per individual were used for statistical analysis where multiple measurements per individual were obtained. Across group comparisons were performed using Student's *t* test and one-way ANOVA. Post-hoc analysis was performed using Tukey's multiple comparisons test. Relationships between variables were

evaluated by performing linear regression and determining the coefficient of determination (R squared, r^2) and correlations were evaluated by determining Pearson's correlation coefficient (r). Significance was set at $P < 0.05$.

Results

Diabetic nephropathy in BTBR *ob*$^{-}$/*ob*$^{-}$ mice is associated with decreased fenestration density, glomerular ultrafiltration coefficient (L_pA/Vi) and GFR, and increased fenestration width.

BTBR *ob*$^{-}$/*ob*$^{-}$ mice at 12 to 20 weeks of age demonstrated increased body weight, hyperglycaemia and albuminuria, compared to littermate control mice confirming development of diabetes and diabetic nephropathy (Figure 1A,B,C). Podocyte slit diaphragm density was significantly decreased in diabetic mice whilst podocyte foot process width and GBM thickness were significantly increased (Supplementary information S3), consistent with diabetic nephropathy. Diabetic mice at 20 weeks had significantly decreased endothelial fenestration density (Figure 1D,E) and increased width (Figure 1D,F). L_pA/Vi (Figure 1G) and GFR (Figure 1H) were significantly decreased in diabetic mice, confirming loss of renal filtration function. Glomerular volume (Vi) was not significantly different in diabetic compared to control mice (Supplementary information S3).

Fenestration changes are present from 10 weeks of age in BTBR *ob*$^{-}$/*ob*$^{-}$ mice

GEnC fenestration density was significantly decreased (Figure 2A) whilst GEnC fenestration width was significantly increased (Figure 2B) in diabetic compared to litter mate control mice aged 10, 15 and 20 weeks but not 6 weeks.

Reduction in GEnC fenestration density and increase in width are associated with reduced glomerular ultrafiltration coefficient (L_PA/Vi) and GFR in BTBR *ob*$^-$/*ob*$^-$ mice.

We evaluated the glomerular structural and functional relationships to determine the contribution of GEnC fenestrations to filtration function. There were significant positive correlations between GEnC fenestration density and both L_PA/Vi and GFR (Table 2). Unexpectedly, we identified significant negative correlations between GEnC fenestration width and both L_PA/Vi and GFR. We confirmed there were additional significant positive correlations between podocyte slit width and uACR and GBM thickness and uACR (Table 2) as expected. There were significant negative correlations between podocyte slit density and uACR and GBM width and L_PA/Vi (Table 2). Univariable linear regression and the coefficient of determination (r^2) confirmed significant positive relationships between GEnC fenestration density and both L_PA/Vi (r^2=0.25, P=0.019; Supplementary information S4A) and GFR (r^2=0.27, P=0.020; Supplementary information S4B). There was a significant negative relationship between GEnC width and both L_PA/Vi (r^2=0.33, P=0.007; Supplementary information S4C) and GFR (r^2=21, P=0.041; Supplementary information S4D).

Fenestration surface area is maintained in diabetes, but this is negatively associated with renal filtration function in BTBR *ob*$^{-}$/*ob*$^{-}$ mice.

We next examined if loss of GEnC fenestration density resulted in decreased fenestration surface area that could contribute to reduced renal filtration function. We found that fenestration surface area was maintained in diabetic compared to control mice at 6, 10, 15 and 20 weeks of age (Figure 3A). We postulate that this is due to increased GEnC fenestration width compensating for the loss of GEnC fenestration density in diabetes. There was no significant overall relationship between fenestration surface area and L_PA/Vi (r^2=0.11, P=0.143) and GFR (r^2=0.00, P=0.794). However, when experimental groups were examined separately, we found a positive relationship between fenestration surface area and L_PA/Vi (Figure 3B) in control mice, whereas in diabetic mice the relationship was negative (Figure 3B). These findings suggested reduced hydraulic permeability of GEnC fenestrations in diabetes.

GEnC fenestrations form diaphragms in diabetic nephropathy and this is negatively associated with renal filtration function.

We further studied the presence of diaphragms within the GEnC fenestrations as a potential structural impediment to flow. The percentage of diaphragmed fenestrations was significantly higher (approximately 2-fold) in diabetic mice (Figure 4A,B). There was a significant negative relationship between percentage of diaphragmed fenestrations and L_PA/Vi (Figure 4C). Furthermore, diaphragmed fenestrations were significantly wider in both diabetic and control mice (Figure 4D). We also demonstrated increased expression of the only known component of

fenestral diaphragms, PLVAP at both the protein (Figure 4E,F) and mRNA (Figure 4G) level in diabetic glomeruli, consistent with our TEM findings. There were significant negative correlations between diaphragmed fenestration width and L_PA/Vi (r=-0.56, P=0.011). There was no significant correlation between open fenestration width and L_PA/Vi (r=0.36, P=0.113).

Mathematical modelling to determine the contribution that the glomerular endothelium changes in diabetes make to the observed changes in functional properties of the glomerular capillary wall.

Mathematical modelling which accounted for glomerular endothelial fenestral width, density and diaphragmation, indicated that the total fraction of the capillary surface occupied by all fenestra (E_f) in diabetic mice was 54% of that of control mice (See supplementary information S2).

Eps homology domain protein 3 (Ehd 3) glomerular expression is decreased in diabetes and is associated with GEnC fenestration loss, L_PA/Vi and GFR

Ehd3 is localised to GEnC fenestrations[14] and Ehd3 and 4 knockout mice have complete loss of GEnC fenestrations.[17] We therefore examined Ehd3 expression in diabetes and its association with GEnC fenestral changes and L_PA/Vi. In control mice, Ehd3 colocalised with the endothelial marker CD31 in the glomerulus whilst Ehd4 colocalised with CD31 in the peritubular capillaries (Figure 5A). Glomerular Ehd3 protein expression was significantly decreased in diabetic mice

(Figure 5B,C) whilst mRNA expression was significantly increased (Figure 5D). Ehd3 protein expression was positively associated with fenestration density (r^2=0.52, P<0.0001) and L_PA/Vi (r^2=0.59, P<0.001). Ehd4 glomerular protein (Figure 5B,E) and mRNA (Figure 5F) expression was significantly increased in diabetic mice, perhaps as a compensatory change to loss of Ehd3 expression. There were positive Pearson's correlations between Ehd3 and GFR with negative correlations between Ehd3 and GEnC fenestration width and percentage of diaphragmed fenestrations (Table 3).

GEnC fenestral changes are present in diabetic patients and are associated with eGFR and loss of glomerular EHD3 expression.

Patient demographics, diagnosis and eGFR are presented in supplementary information S6. In biopsy samples from diabetic patients, podocyte slit diaphragm density was significantly decreased in diabetic patients whilst podocyte slit diaphragm width and GBM thickness were significantly increased (Supplementary information S7), consistent with diabetic nephropathy. GEnC fenestration density was significantly decreased (Figure 6A,B) and fenestration width significantly increased (Figure 6A,C). However, in contrast to diabetic mice, the fenestration surface area was significantly decreased in diabetic compared to control samples (Figure 6D). As with diabetic mice, we found there were significant positive Pearson's correlations between GEnC fenestration density and eGFR and between fenestration surface area and eGFR (Table 4). There were significant negative correlations between GEnC fenestration width and eGFR and

GBM thickness and eGFR. There were no significant relationships between podocyte measurements and eGFR.

We identified significantly decreased glomerular capillary EHD3 expression (Figure 6E,F) in diabetic samples. eGFR measurements were available for 4 control and 5 diabetic patients. There was a significant positive relationship between EHD3 and eGFR (r^2=0.42, P=0.047).

Nephroseq datasets were extracted to further examine glomerular EHD3 and PLVAP (as an index of diaphragmed fenestrations) expression in diabetic patient cohorts. PLVAP expression in the Nephroseq 'Ju CKD Glom' dataset was examined. There was significantly increased median-centered Log2 PLVAP expression in glomeruli of diabetic compared to control healthy living donor patients (Figure 7A) and a significant negative relationship with eGFR (Figure 7B), suggesting there was increased diaphragmed fenestrations present in human diabetic patients and that this may be contributing to resistance to filtration function. In addition, glomerular EHD3 expression was studied in the Nephroseq 'Woroniecka Diabetes Glom' dataset. There was significantly decreased median-centered Log2 EHD3 expression in glomeruli of diabetic compared to control healthy living donor patients (Figure 7C) and a significant positive relationship with eGFR (Figure 7D). Further analysis of the Nephroseq database revealed that renal EHD3 expression was significantly decreased in other kidney diseases (Table 5), including chronic kidney disease and focal segmental glomerulosclerosis.

Ehd3 knockdown decreases fenestration formation in a fenestration forming endothelial cell line

The associations between Ehd3 and GEnC fenestration ultrastructural measurements suggested Ehd3 may directly regulate fenestrations thereby influencing GFR. We further examined the role of Ehd3 in fenestration regulation by knocking down Ehd3 in a fenestration forming cell line (mouse brain endothelioma cells; b.End5[18, 19]) (Figure 8A,B,C). Fenestration formation was significantly decreased in Ehd3 knockdown cells in response to Latrunculin A, an actin depolymerising agent (Figure 8D,E). There was a complete absence of fenestration formation in Ehd3 knockdown cells in response to mouse $VEGF_{164}$ (Figure 8D,E). Ehd3 knockdown did not have any significant effect on fenestration width in response to Latrunculin A (Figure 8D,F). Fenestrations formed in control cells in response to $VEGF_{164}$ were significantly wider (Figure 8D,F) with the appearance of being less organised within sieve plates compared to fenestrations formed in response to Latrunculin A (Figure 8D).

Discussion

In this study, we examine the role of GEnC fenestrations in GFR loss in diabetic nephropathy. We comprehensively characterised GEnC ultrastructural changes in diabetic nephropathy and examined relationships with renal filtration function. We further studied glomerular EHD3 expression in diabetes and demonstrated that its loss *in vitro* results in decreased fenestration formation. We identified decreased GEnC fenestration density, L_pA/Vi and GFR and increased GEnC fenestration width in a mouse model of diabetic nephropathy and also diabetic patients.

We observed positive relationships between fenestration density and renal filtration measurements, indicating that as fenestrations are lost, renal filtration function declines. The contribution of GEnC fenestration density to renal filtration function likely has relevance to other kidney diseases that are characterised by declining GFR. It is well established that women with pre-eclampsia (a form of thrombotic microangiopathy) have a marked endothelial phenotype with GEnC fenestration loss, and this is considered to contribute to decreased GFR.[20] In liver sinusoidal endothelial cells, with non-diaphragmed fenestrated endothelium that most closely resembles GEnC fenestrae, fenestration loss is associated with aging[21-23] and is a proposed mechanism for dyslipidaemia in elderly people. It is therefore possible that age related decline in GFR might also be related to loss of GEnC fenestrations. It has also been demonstrated that in diabetic nephropathy the percentage of glomerular endothelial cells in the total glomerular cell population increases[24] and therefore, the importance of these cells and their associated fenestrations may become even more relevant.

Mathematical modelling based on the normal fenestrated glomerular capillary morphology indicates that the contribution of the glomerular endothelium to resistance to hydraulic permeability at the glomerular filtration barrier is neglible.[6] However, this modelling did not account for the presence of diaphragms in fenestrations.[6] The findings of the present study show an association between increased percentage of diaphragmed fenestrations and LpA/Vi and we suggest that diaphragmed fenestrations may contribute to glomerular hydraulic permeability resistance. The relationships identified in the present study between GEnC fenestration density and both L_PA/Vi and GFR support the supposition that these structures

play an important role in limiting filtration function. Further, mathematical modelling of the glomerular endothelial fenestral changes that contribute to the functional properties of the glomerulus was performed. To our knowledge there are no other models that have incorporated the contribution of the development of diaphragms in GEnC fenestrations. The data in our paper demonstrates that there were no significant differences in fenestration surface area and glomerular volume (Vi) between control and diabetic glomeruli and hence observed changes in the glomerular ultrafiltration coefficient (LpA/Vi) likely reflect changes in hydraulic permeability rather than changes in surface area-dependent terms. The glomerular ultrafiltration coefficient was 54% of control values in diabetic mice. The observed changes in endothelial dimensions, when applied to basic mathematical modelling, were in the same direction and of the same order of magnitude (54%) as the observed change in glomerular ultrafiltration coefficient (LpA/Vi). There are inherent limitations of mathematical models including failure to accommodate key ultrastructural features such as those identified in this manuscript (fenestral diaphragms, variable fenestral width), assumptions about biophysical properties such as fenestrae being fluid filled and somewhat arbitrary percentages of overall flow resistance ascribed to the cells and to the GBM. However, the mathematical modelling we performed does indicate a change in key endothelial determinants of hydraulic resistance. The glomerular ultrafiltration coefficient measurements provide an important measured functional correlate of these mathematical predictions. Other structural determinants of hydraulic permeability at the glomerular filtration barrier include the GBM, endothelial junctional integrity, podocyte slit diaphragm, slit process width and density and endothelial and epithelial glycocalyx. In the present study, there was a significant correlation between GBM and LpA/Vi

and, GBM width was significantly increased in diabetic mice and patients. Therefore, we cannot exclude that increased GBM thickness was a confounder in the findings of our study. Relationships between podocyte measurements and L_PA/Vi were not statistically significant. However, podocyte slit width and density and GBM width were correlated with uACR whilst fenestral measurements were not. The study findings suggest that GEnC fenestrae and GBM play a predominant role in regulating hydraulic permeability but that podocytes and GBM are more important regulators of albumin permeability at the glomerular filtration barrier.

BTBR *ob*$^{-/}$*ob*$^{-}$ mice become hyperglycaemic from 3 weeks[25] and albuminuric from 8 weeks of age.[12] We describe the glomerular ultrastructural findings in this model for the first time and demonstrate decreased GEnC fenestration density and increased width in BTBR *ob*$^{-/}$*ob*$^{-}$ by 10 weeks of age. We further demonstrated loss of renal filtration function in this model including (LpA/Vi) and GFR. However, it must be noted that GFR was determined by measurement of endogenous creatinine clearance that is associated with some limitations in mice such as tubular secretion of creatinine. GEnC fenestration width is greater in diabetic rats compared to control rats[26] consistent with the findings of this study. In the present study, increased GEnC fenestration width with decreasing GEnC fenestration density maintained the GEnC fenestration surface area in diabetic mice. In contrast to mice, human diabetic patients had significantly decreased GEnC fenestration surface area despite increased GEnC fenestration width. This likely reflects a later stage of disease in diabetic patients in which increased GEnC fenestration width cannot compensate for the loss of GEnC fenestration density to maintain fenestration surface area. Indeed, mean GEnC fenestration density was lower in human diabetic

patients compared to diabetic mice. Measurement of renal filtration functional change at different stages of disease in addition to evaluating the GEnC fenestral changes may provide useful information regarding disease course.

Despite maintenance of fenestration surface area there was loss of filtration function in diabetic mice. Unexpectedly, we also identified a significant negative relationship between GEnC fenestration width and L_PA/Vi. We postulated that this may be due to the development of diaphragms in the GEnC fenestrations providing resistance to hydraulic permeability. The number of diaphragmed fenestrae is approximately 4 times greater in GEnC recovering from injury[27] suggesting a possible role in remodelling. In addition, increased glomerular capillary PLVAP, the only known component of diaphragms, expression is reported in injured glomeruli.[27] We observed significantly increased diaphragmed fenestrations in diabetic mice. Furthermore, we identified increased glomerular PLVAP in diabetic mice and humans. We also observed diaphragmed fenestrations to have increased width compared to open fenestrations, suggesting diaphragms develop in widening GEnC fenestrations. It has been proposed that upregulation of PLVAP and development of diaphragms in reconstructing capillaries may involve VEGF.[27] Glomerular VEGF signalling is altered in diabetes.[28] The role of VEGF in PLVAP upregulation and formation of diaphragmed fenestrae in GEnC remains to be explored. It has also been speculated that diaphragmed fenestrations provide some form of structural support or controlled permeability.[29] We identified a significant negative relationship between percentage of diaphragmed GEnC fenestrations and L_PA/Vi in mice and PLVAP expression with eGFR in humans. This suggests the presence of diaphragms in GEnC fenestrations may provide

resistance to glomerular hydraulic permeability. It is also possible that the endothelial glycocalyx may be contributing to fenestral resistance.[30] Importantly, we suggest that the fenestration surface area cannot be considered the filtration surface area as the contribution that each individual fenestrae will make to hydraulic permeability will not be equal due to variations in diaphragmation and glycocalyx composition. Further, that the absence of diaphragms in GEnC is likely to be critical in supporting the high hydraulic permeability required for renal filtration function.

We demonstrate decreased glomerular EHD3 protein expression in diabetic mice and humans. Principle component analysis of glomerular endothelial cells from BTBR $ob^{-/}ob^{-}$ mice showed modest transcriptional changes (compared to those seen in podocytes or mesangial cells) acknowledged to be an unexpected finding,[16] but individual gene changes e.g. in EHD3, were not reported. Whether any structural or functional change was present in this population of mice was also not described.[16]

Analysing data from the kidney transcriptomics database Nephroseq, we also identified significantly decreased glomerular EHD3 expression in diabetic patients. In the present study associations between glomerular EHD3 expression and GEnC fenestral measurements were identified. Furthermore, loss of EHD3 expression was associated with decreased L_PA/Vi and GFR possibly due to changes in GEnC fenestrations. Using Nephroseq datasets we also identified decreased EHD3 in other kidney diseases including chronic kidney disease (CKD). It is therefore possible that loss of glomerular EHD3 expression may contribute to GEnC fenestral changes,

resulting in decreased L_pA/Vi, in other kidney diseases characterised by declining GFR. We demonstrated increased glomerular EHD4 protein expression in diabetic mice and human patients. An increase in glomerular capillary Ehd4 expression has been demonstrated in Ehd3 knockout mice.[17] Increased Ehd4 expression has also been demonstrated in skeletal muscle in Ehd1 knockout mice.[31] This suggests increases in EHD paralogs may be a possible compensatory mechanism for decreased expression of another. Both knockdown of Ehd3 and 4 is required to see a marked glomerular endothelial phenotype with absence of fenestrations.[17] A quantitative comparison of fenestration density or width in $Ehd3^{-/-}/Ehd4^{-/-}$ and $Ehd3^{-/-}/Ehd4^{+/+}$ mice was not undertaken in this previous study.[17]

Due to the role of EHD3 in endocytic trafficking, it has been postulated that it may regulate recycling and membrane availability of vascular endothelial growth factor receptor 2 (VEGFR2) resulting in altered VEGF signaling.[17] VEGF-A has a critical role in GEnC fenestration regulation.[5, 32, 33] It is also possible that EHD3 regulates GEnC fenestrations via other mechanisms such as indirectly via endocytic recycling of other angiogenic factors or directly via interactions with the cellular cytoskeleton. However, EHD3 does not associate with actin microfilaments and treatment with cytochalasin D, an actin polymerising inhibitor, does not result in altered EHD3 cellular location.[34] The *in vitro* EHD3 knockdown data in the present study supported the postulation that EHD3 plays a role in regulating fenestration formation. The findings also support the supposition that endocytic recycling of VEGFR2 is the predominant mechanism by which EHD3 regulates fenestrations. EHD3 knockdown cells demonstrated complete absence of fenestration formation in response to VEGF-A whilst fenestration density was decreased in

response to latrunculin, an actin depolymerising agent. A limitation of the *in vitro* EHD3 knockdown studies is that it was not possible to perform these in GEnC lines as these do not readily form sieve plates. Furthermore, we cannot exclude that by inactivating EHD3, there are nonspecific changes within the cell.

In summary, we demonstrated loss of GEnC fenestration density associated with decreased L_pA/Vi and GFR in diabetic nephropathy. GEnC fenestration width increased, an ultrastructural change that may occur to maintain fenestration surface area. GEnC fenestration width was negatively associated with L_pA/Vi and GFR. This was posited to be a result of the development of diaphragms in widening fenestrations providing structural resistance. Glomerular EHD3 expression decreases in diabetes and its association with GEnC fenestration measurements suggests it may play a role in regulating fenestrations. This was supported by knocking down EHD3 in a fenestration forming cell line resulting in absence of or decreased fenestration formation. Loss of glomerular EHD3 expression in disease may contribute to declining glomerular filtration function through aberrant GEnC fenestration regulation. These results suggest that targeted therapies to restore GEnC fenestrations potentially by manipulating glomerular EHD3 expression may offer potential for restoring renal filtration function in diabetic nephropathy as well as other chronic kidney diseases characterised by similar aberrations in GEnC fenestration regulation and loss of glomerular EHD3 expression.

Author contributions

CRediT Taxonomy

Natalie Finch: Conceptualization, Data curation, Formal analysis, Funding acquisition, Investigation, Methodology, Project administration, Resources, Supervision, Validation, Visualization, Writing – original draft, Writing – review & editing

Sarah Fawaz: Data curation, Formal analysis, Methodology, Writing – original draft, Writing – review & editing

Christopher Neal: Data curation, Formal analysis, Investigation, Methodology, Visualization, Writing – original draft, Writing – review & editing

Matthew Butler: Resources, Writing – review & editing

Vivian Lee: Investigation, Resources, Writing – review & editing

Andrew Salmon: Formal analysis, Methodology, Writing – review & editing

Abigail Lay: Methodology, Writing – review & editing

Megan Stevens: Methodology, Writing – review & editing

Lusyan Dalayan: Formal analysis, Writing – review & editing

Hamid Band: Resources, Writing – review & editing

Harry Mellor: Methodology, Resources, Writing – review & editing

Steven Harper: Project administration

David Shima: Funding acquisition, Methodology, Resources, Writing – review & editing

Gavin Welsh: Conceptualization, Formal analysis, Investigation, Methodology, Supervision, Writing – original draft, Writing – review & editing

Rebecca Foster: Conceptualization, Formal analysis, Funding acquisition, Investigation, Methodology, Supervision, Writing – original draft, Writing – review & editing

Simon Satchell: Conceptualization, Formal analysis, Funding acquisition, Investigation, Methodology, Resources, Supervision, Writing – original draft, Writing – review & editing

Acknowledgements

The authors would like to acknowledge the Wolfson Bioimaging Facility, University of Bristol for providing imaging support and Translational Vision Research Laboratory, University College London for training in inducing fenestrations in b.End5 and the Cellular Pathology Department, North Bristol NHS trust for providing patient kidney samples.

Funding: This research was funded in whole, or in part, by the Wellcome Trust [104507/Z/14/Z].

Disclosures:

N. Finch reports Research Funding: Boehringer Animal Health; and Scientific Advisor or Membership: Governing Council of the Cat Fancy. A. Salmon reports Advisory or Leadership Role: Kidney Health New Zealand. H. Band reports Patents and Inventions: EMD-Millipore,

Amgen (one time), and Genentech (one time). S. Harper reports Consultancy: Exonate Ltd; Ownership Interest: Exonate Ltd, Emenda Therapeutics Ltd, Four Rivers Renal Services Ltd, Patents or Royalties: Via University of Bristol revenue sharing; and Advisory or Leadership Role: Exonate Ltd Board Member & Co-Founder, Emenda Therapeutics Board Member & Co-Founder, Four Rivers Renal Services Board Member and Founder. D. Shima reports Scientific Advisor or Membership: American Journal of Pathology Editorial Board G. Welsh reports Consultancy Agreements: Purespring Therapeutics; and Research Funding: Travere Therapeutics. S. Satchell reports Consultancy Agreements: Novo Nordisk, Research Funding: Ferring, Evotec, Novo Nordisk; Scientific Advisor or Membership: Kidney Research UK Grants Committee; and Other Interests/Relationships: Member of the UK Kidney Association.

Supplementary material table of contents

Supplementary information S4: Reduction in GEnC fenestration density and increase in width are associated with reduced glomerular ultrafiltration coefficient and GFR in BTBR *ob*$^{-}$/*ob*$^{-}$ mice.

Supplementary information S5: Pearson's correlation between glomerular Ehd3 and Ehd4 expression and podocyte and GBM measurements.

Supplementary information S6: Patient demographics, diagnosis and eGFR.

Supplementary information S7: Podocyte and glomerular basement membrane measurements confirming developing of diabetic nephropathy in human diabetic patients.

Supplementary information S8: Glomerular EHD4 expression is significantly increased in human diabetic patients compared to controls.

References

1. Satchell, SC, Braet, F: Glomerular endothelial cell fenestrations: an integral component of the glomerular filtration barrier. *Am J Physiol Renal Physiol,* 296**:** F947-956, 2009.
2. Salmon, AH, Neal, CR, Bates, DO, Harper, SJ: Vascular endothelial growth factor increases the ultrafiltration coefficient in isolated intact Wistar rat glomeruli. *J Physiol,* 570**:** 141-156, 2006.
3. Oltean, S, Qiu, Y, Ferguson, JK, Stevens, M, Neal, C, Russell, A, Kaura, A, Arkill, KP, Harris, K, Symonds, C, Lacey, K, Wijeyaratne, L, Gammons, M, Wylie, E, Hulse, RP, Alsop, C, Cope, G, Damodaran, G, Betteridge, KB, Ramnath, R, Satchell, SC, Foster, RR, Ballmer-Hofer, K, Donaldson, LF, Barratt, J, Baelde, HJ, Harper, SJ, Bates, DO, Salmon, AH: Vascular Endothelial Growth Factor-A165b Is Protective and Restores Endothelial Glycocalyx in Diabetic Nephropathy. *J Am Soc Nephrol,* 26**:** 1889-1904, 2015.
4. Stevens, M, Neal, CR, Salmon, AHJ, Bates, DO, Harper, SJ, Oltean, S: Vascular Endothelial Growth Factor-A165b Restores Normal Glomerular Water Permeability in a Diphtheria-Toxin Mouse Model of Glomerular Injury. *Nephron,* 139**:** 51-62, 2018.

5. Qiu, Y, Ferguson, J, Oltean, S, Neal, CR, Kaura, A, Bevan, H, Wood, E, Sage, LM, Lanati, S, Nowak, DG, Salmon, AH, Bates, D, Harper, SJ: Overexpression of VEGF165b in podocytes reduces glomerular permeability. *J Am Soc Nephrol,* 21**:** 1498-1509, 2010.
6. Drumond, MC, Deen, WM: Structural determinants of glomerular hydraulic permeability. *Am J Physiol,* 266**:** F1-12, 1994.
7. Lafayette, RA, Druzin, M, Sibley, R, Derby, G, Malik, T, Huie, P, Polhemus, C, Deen, WM, Myers, BD: Nature of glomerular dysfunction in pre-eclampsia. *Kidney Int,* 54**:** 1240-1249, 1998.
8. Alicic, RZ, Rooney, MT, Tuttle, KR: Diabetic Kidney Disease: Challenges, Progress, and Possibilities. *Clin J Am Soc Nephrol,* 12**:** 2032-2045, 2017.
9. Weil, EJ, Lemley, KV, Mason, CC, Yee, B, Jones, LI, Blouch, K, Lovato, T, Richardson, M, Myers, BD, Nelson, RG: Podocyte detachment and reduced glomerular capillary endothelial fenestration promote kidney disease in type 2 diabetic nephropathy. *Kidney Int,* 82**:** 1010-1017, 2012.
10. Fufaa, GD, Weil, EJ, Lemley, KV, Knowler, WC, Brosius, FC, 3rd, Yee, B, Mauer, M, Nelson, RG: Structural Predictors of Loss of Renal Function in American Indians with Type 2 Diabetes. *Clin J Am Soc Nephrol,* 11**:** 254-261, 2016.
11. Toyoda, M, Najafian, B, Kim, Y, Caramori, ML, Mauer, M: Podocyte detachment and reduced glomerular capillary endothelial fenestration in human type 1 diabetic nephropathy. *Diabetes,* 56**:** 2155-2160, 2007.
12. Hudkins, KL, Pichaiwong, W, Wietecha, T, Kowalewska, J, Banas, MC, Spencer, MW, Muhlfeld, A, Koelling, M, Pippin, JW, Shankland, SJ, Askari, B, Rabaglia, ME, Keller, MP, Attie, AD, Alpers, CE: BTBR Ob/Ob mutant mice model progressive diabetic nephropathy. *J Am Soc Nephrol,* 21**:** 1533-1542, 2010.
13. Grant, BD, Caplan, S: Mechanisms of EHD/RME-1 protein function in endocytic transport. *Traffic,* 9**:** 2043-2052, 2008.
14. Patrakka, J, Xiao, Z, Nukui, M, Takemoto, M, He, L, Oddsson, A, Perisic, L, Kaukinen, A, Szigyarto, CA, Uhlen, M, Jalanko, H, Betsholtz, C, Tryggvason, K: Expression and subcellular distribution of novel glomerulus-associated proteins dendrin, ehd3, sh2d4a, plekhh2, and 2310066E14Rik. *J Am Soc Nephrol,* 18**:** 689-697, 2007.
15. Karaiskos, N, Rahmatollahi, M, Boltengagen, A, Liu, H, Hoehne, M, Rinschen, M, Schermer, B, Benzing, T, Rajewsky, N, Kocks, C, Kann, M, Muller, RU: A Single-Cell Transcriptome Atlas of the Mouse Glomerulus. *J Am Soc Nephrol,* 29**:** 2060-2068, 2018.
16. Chung, JJ, Goldstein, L, Chen, YJ, Lee, J, Webster, JD, Roose-Girma, M, Paudyal, SC, Modrusan, Z, Dey, A, Shaw, AS: Single-Cell Transcriptome Profiling of the Kidney Glomerulus Identifies Key Cell Types and Reactions to Injury. *J Am Soc Nephrol,* 31**:** 2341-2354, 2020.
17. George, M, Rainey, MA, Naramura, M, Foster, KW, Holzapfel, MS, Willoughby, LL, Ying, G, Goswami, RM, Gurumurthy, CB, Band, V, Satchell, SC, Band, H: Renal thrombotic microangiopathy in mice with combined deletion of endocytic recycling regulators EHD3 and EHD4. *PLoS One,* 6**:** e17838, 2011.
18. Ioannidou, S, Deinhardt, K, Miotla, J, Bradley, J, Cheung, E, Samuelsson, S, Ng, YS, Shima, DT: An in vitro assay reveals a role for the diaphragm protein PV-1 in endothelial fenestra morphogenesis. *Proc Natl Acad Sci U S A,* 103**:** 16770-16775, 2006.

19. Ju, M, Ioannidou, S, Munro, P, Ramo, O, Vihinen, H, Jokitalo, E, Shima, DT: A Na,K-ATPase-Fodrin-Actin Membrane Cytoskeleton Complex is Required for Endothelial Fenestra Biogenesis. *Cells,* 9, 2020.
20. Stillman, IE, Karumanchi, SA: The glomerular injury of preeclampsia. *J Am Soc Nephrol,* 18**:** 2281-2284, 2007.
21. Hilmer, SN, Cogger, VC, Fraser, R, McLean, AJ, Sullivan, D, Le Couteur, DG: Age-related changes in the hepatic sinusoidal endothelium impede lipoprotein transfer in the rat. *Hepatology,* 42**:** 1349-1354, 2005.
22. Le Couteur, DG, Cogger, VC, Markus, AM, Harvey, PJ, Yin, ZL, Ansselin, AD, McLean, AJ: Pseudocapillarization and associated energy limitation in the aged rat liver. *Hepatology,* 33**:** 537-543, 2001.
23. Hunt, NJ, Lockwood, GP, Warren, A, Mao, H, McCourt, PAG, Le Couteur, DG, Cogger, VC: Manipulating fenestrations in young and old liver sinusoidal endothelial cells. *American journal of physiology Gastrointestinal and liver physiology,* 316**:** G144-G154, 2019.
24. Fu, J, Akat, KM, Sun, Z, Zhang, W, Schlondorff, D, Liu, Z, Tuschl, T, Lee, K, He, JC: Single-Cell RNA Profiling of Glomerular Cells Shows Dynamic Changes in Experimental Diabetic Kidney Disease. *J Am Soc Nephrol,* 30**:** 533-545, 2019.
25. Lee, VK, Hosking, BM, Holeniewska, J, Kubala, EC, Lundh von Leithner, P, Gardner, PJ, Foxton, RH, Shima, DT: BTBR ob/ob mouse model of type 2 diabetes exhibits early loss of retinal function and retinal inflammation followed by late vascular changes. *Diabetologia,* 61**:** 2422-2432, 2018.
26. Paeng, J, Park, J, Um, JE, Nam, BY, Kang, HY, Kim, S, Oh, HJ, Park, JT, Han, SH, Ryu, DR, Yoo, TH, Kang, SW: The locally activated renin-angiotensin system is involved in albumin permeability in glomerular endothelial cells under high glucose conditions. *Nephrol Dial Transplant,* 32**:** 61-72, 2017.
27. Ichimura, K, Stan, RV, Kurihara, H, Sakai, T: Glomerular endothelial cells form diaphragms during development and pathologic conditions. *J Am Soc Nephrol,* 19**:** 1463-1471, 2008.
28. Tufro, A, Veron, D: VEGF and podocytes in diabetic nephropathy. *Semin Nephrol,* 32**:** 385-393, 2012.
29. Stan, RV, Tse, D, Deharvengt, SJ, Smits, NC, Xu, Y, Luciano, MR, McGarry, CL, Buitendijk, M, Nemani, KV, Elgueta, R, Kobayashi, T, Shipman, SL, Moodie, KL, Daghlian, CP, Ernst, PA, Lee, HK, Suriawinata, AA, Schned, AR, Longnecker, DS, Fiering, SN, Noelle, RJ, Gimi, B, Shworak, NW, Carriere, C: The diaphragms of fenestrated endothelia: gatekeepers of vascular permeability and blood composition. *Dev Cell,* 23**:** 1203-1218, 2012.
30. Levick, JR, Smaje, LH: An analysis of the permeability of a fenestra. *Microvasc Res,* 33**:** 233-256, 1987.
31. Mate, SE, Van Der Meulen, JH, Arya, P, Bhattacharyya, S, Band, H, Hoffman, EP: Eps homology domain endosomal transport proteins differentially localize to the neuromuscular junction. *Skelet Muscle,* 2**:** 19, 2012.
32. Eremina, V, Sood, M, Haigh, J, Nagy, A, Lajoie, G, Ferrara, N, Gerber, HP, Kikkawa, Y, Miner, JH, Quaggin, SE: Glomerular-specific alterations of VEGF-A expression lead to distinct congenital and acquired renal diseases. *J Clin Invest,* 111**:** 707-716, 2003.

33. Stevens, M, Neal, CR, Salmon, AHJ, Bates, DO, Harper, SJ, Oltean, S: VEGF-A165 b protects against proteinuria in a mouse model with progressive depletion of all endogenous VEGF-A splice isoforms from the kidney. *J Physiol,* 595**:** 6281-6298, 2017.
34. Galperin, E, Benjamin, S, Rapaport, D, Rotem-Yehudar, R, Tolchinsky, S, Horowitz, M: EHD3: a protein that resides in recycling tubular and vesicular membrane structures and interacts with EHD1. *Traffic,* 3**:** 575-589, 2002.

Tables

Table 1: List of antibodies

Antibody	Host species	Dilution	Manufacturer and product number	Samples applied to
Ehd3	Rabbit	1:100	Kindly gifted from Dr Hamid Band, University of Nebraska	Mouse, b.End5
Ehd4	Rabbit	1:100	Kindly gifted from Dr Hamid Band, University of Nebraska	Mouse
EHD3	Rabbit	1:50	Novus NBP2-31894	Human
EHD4	Rabbit	1:50	Proteintech 11382-2-AP	Human
PLVAP	Rat	1:50	Santa Cruz sc-19603	Mouse

Table 2: Pearson's correlation between glomerular ultrastructural and functional measurements. GEnC, glomerular endothelial cell; LpA/Vi, Glomerular ultrafiltration coefficient; GFR, glomerular filtration rate; uACR, urinary albumin creatinine ratio; * $P < 0.05$; ** $P < 0.01$.

	LpA/Vi	GFR	uACR
GEnC fenestration density	0.50*	0.52*	-0.19
GEnC fenestration width	-0.57**	-0.46*	0.41
Podocyte slit density	0.39	0.38	-0.52*
Podocyte slit width	-0.42	-0.24	0.65**
Podocyte foot process width	-0.09	-0.30	0.10
Glomerular basement membrane width	-0.53*	-0.35	0.54*

Table 3: Pearson's correlation between Ehd3 and Ehd4 expression and GEnC fenestral, fenestration surface area and functional measurements. GEnC, glomerular endothelial cell; LpA/Vi, Glomerular ultrafiltration coefficient; GFR, glomerular filtration rate; * P <0.05; ** P <0.01; *** P <0.001; **** P < 0.0001.

	GEnC fenestration density	GEnC fenestration width	% Diaphragmed fenestrations	Fenestration surface area	LpA/Vi	GFR
Ehd3	0.72***	-0.82****	-0.65**	-0.12	0.77***	0.57*
Ehd4	-0.62**	0.64**	0.72***	0.12	-0.60**	-0.47

Table 4: Pearson's correlation between glomerular ultrastructural and eGFR measurements in human patients. eGFR, estimated glomerular filtration rate; * P <0.05; ** P<0.01.

	eGFR
GEnC fenestration density	0.77**
GEnC fenestration width	-0.62*
Fenestration surface area	0.71*
Podocyte slit density	0.46
Podocyte slit width	-0.43
Podocyte foot process width	-0.03
Glomerular basement membrane width	-0.83**

Table 5: Decreased kidney EHD3 expression (median-centered Log2 expression value) in other kidney diseases compared to control patients. Data extracted from Nephroseq database (www.nephroseq.org). † Nakagawa CKD kidney dataset; †† Hodgin FSGS glom dataset

Disease comparison	P value	Fold change
CKD vs normal kidney†	$4.08e^{-4}$	-11.230
Collapsing Focal Segmental Glomerulosclerosis vs normal kidney††	0.003	-2.285

Figure 1: Diabetic nephropathy in BTBR *ob*$^{-}$/*ob*$^{-}$ mice is associated with decreased fenestration density, glomerular ultrafiltration coefficient (L_pA/Vi) and GFR and increased fenestration width.

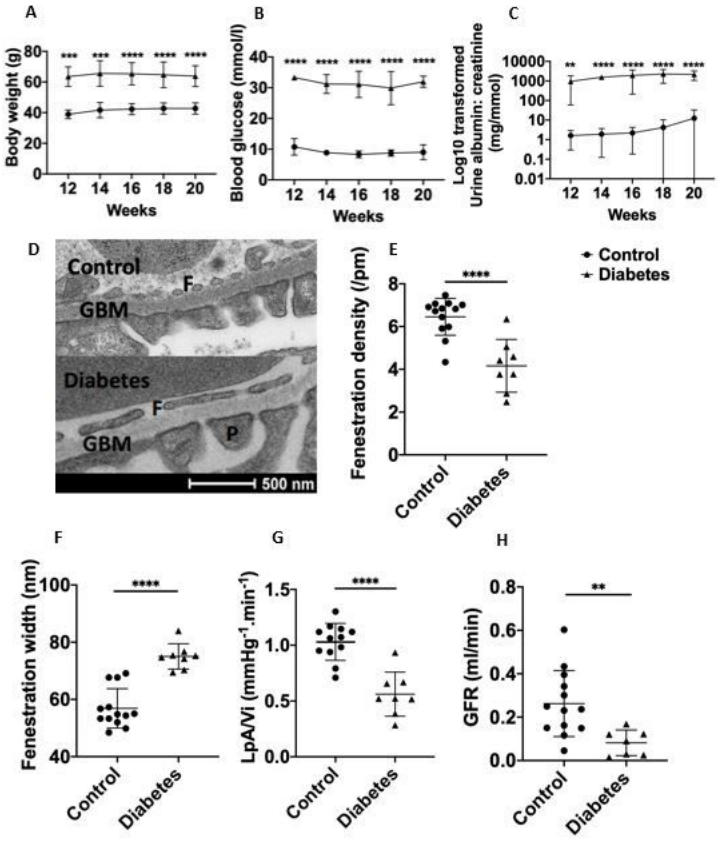

Body weight (A), blood glucose (B) and uACR (C) in BTBR *ob*$^{-}$/*ob*$^{-}$ mice (n=8) compared to litter mate control mice (BTBR *ob*$^{+}$/*ob*$^{+}$; n=13). Bodyweight, blood glucose and uACR was significantly increased in BTBR *ob*$^{+}$/*ob*$^{+}$ at all time points confirming development of diabetes and diabetic nephropathy. Representative transmission electron micrograph demonstrating loss of fenestration density in diabetic mice aged 20 weeks (D). At 20 weeks of age fenestration density (E) was significantly decreased and fenestration width increased (F) in diabetic (n=8) compared to control mice (n=13). Glomerular ultrafiltration coefficient (G; L_pA/V_i) was also significantly decreased in diabetic compared to control mice. GFR (H) was significantly decreased in diabetic (n=7) compared to control mice (n=13). ns, not significant; ** P <0.01; *** P <0.001; **** P <0.0001.

Figure 2: Fenestration changes are present from 10 weeks of age in BTBR *ob*$^{-}$/*ob*$^{-}$ mice.

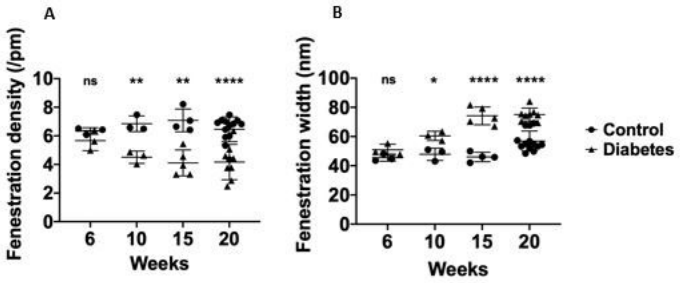

GEnC fenestration density was significantly decreased in diabetic compared to litter mate control mice aged 10, 15 and 20 weeks but not 6 weeks (A). GEnC fenestration width was significantly increased in diabetic compared to litter mate control mice aged 10, 15 and 20 weeks but not 6 weeks (B). F, GEnC fenestration; GBM, glomerular basement membrane; P, podocyte foot process; ns, not significant; ** $P < 0.01$; **** $P < 0.0001$.

Figure 3: Fenestration surface area is maintained in diabetes, but this is negatively associated with renal filtration function in diabetes in BTBR *ob*$^{-}$/*ob*$^{-}$ mice.

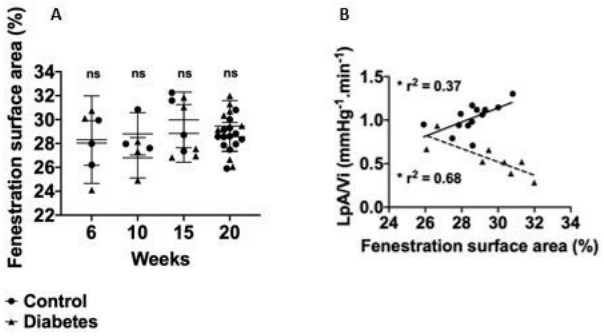

Fenestration surface area was not significantly different in diabetic compared to control mice aged 6, 10, 15 and 20 weeks (A). There was a significant positive relationship between fenestration surface area and glomerular ultrafiltration coefficient (B) in control mice whereas in diabetic mice the relationship was negative (B). Bold line indicates line of regression for control mice (B) and dashed line indicates line of regression for diabetic mice (B). * P <0.05.

Figure 4: GEnC fenestrations form diaphragms in diabetic nephropathy and this is negatively associated with renal filtration function in BTBR *ob*$^{-}$/*ob*$^{-}$ mice.

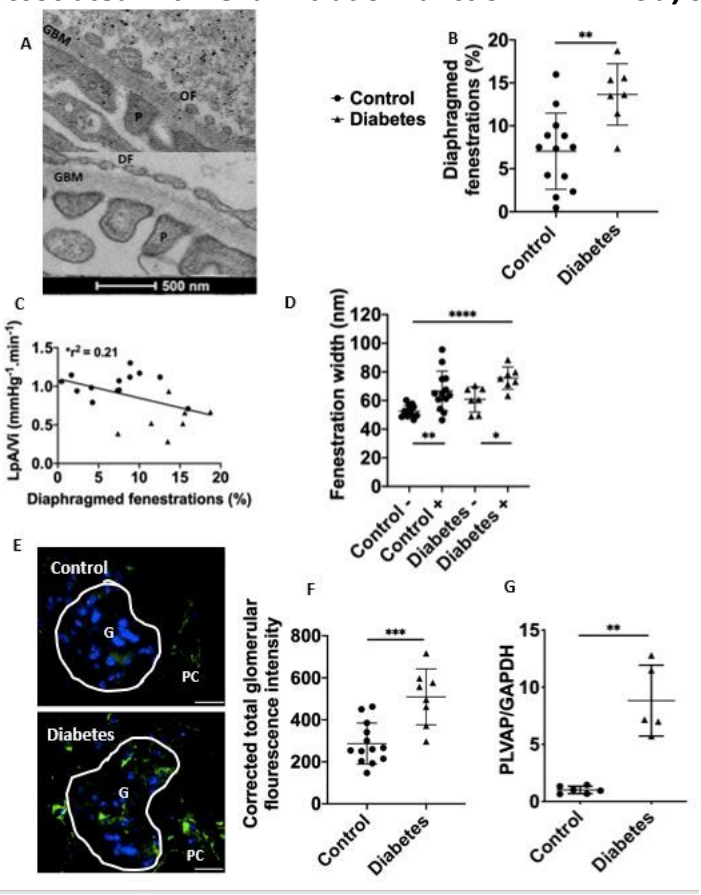

Representative TEM images demonstrating the presence of diaphragmed fenestrations in diabetic mice and open fenestrations in control mice (A). The percentage of diaphragmed fenestrations was significantly increased in diabetic compared to litter mate control mice (B). There was a significant negative relationship between the percentage of diaphragmed fenestrations and glomerular ultrafiltration coefficient (L_PA/V_i;C). Fenestration width was significantly higher in diaphragmed fenestrations in both diabetic and control mice (D). Representative image of glomerular PLVAP1 expression determined by immunofluorescence (E). PLVAP1 protein (F) and mRNA (G) glomerular expression was significantly increased in diabetic compared to control mice. Bold line indicates line of regression for all data points in (C); Scale bars 25µm (E); OF, open fenestration; DF, diaphragmed fenestration; GBM, glomerular basement membrane; P, podocyte foot process (A); Control -, control open fenestrations; Control +, control diaphragmed fenestrations; Diabetes -, diabetes open fenestrations; Diabetes +, diabetes diaphragmed fenestrations (D); G, glomerulus; PC, peritubular capillary (E); * P <0.05, ** P <0.01, *** P <0.001, *** P <0.0001.

Figure 5: **Eps homology domain proteins 3 and 4 (Ehd 3 and 4) expression is altered in diabetes and is associated with GEnC fenestration loss, L_pA/Vi and GFR.**

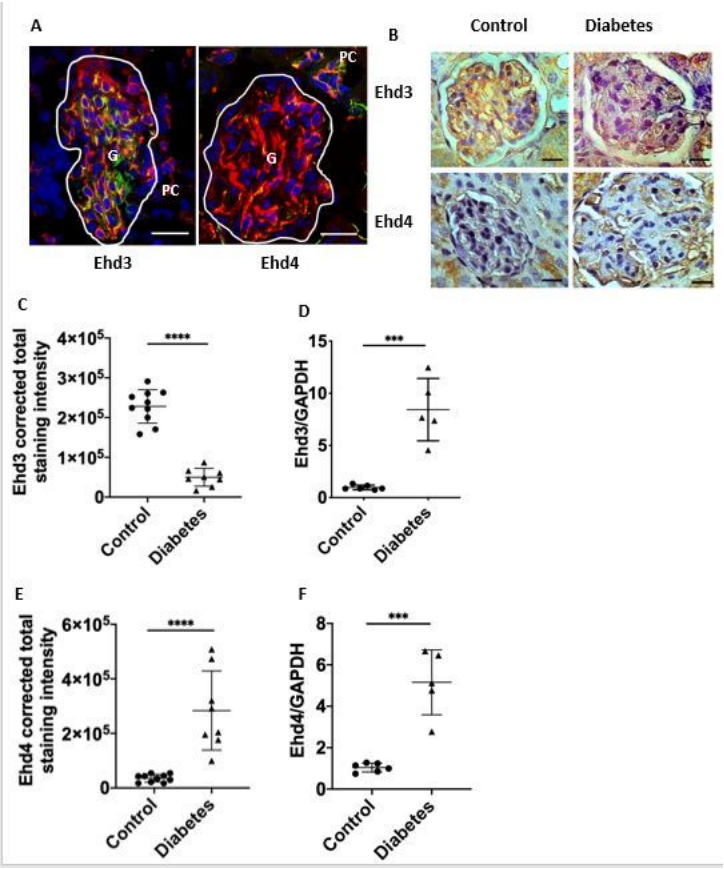

Representative immunofluorescence images demonstrating colocalization of Ehd3 and 4 (green) with the endothelial marker CD31 (red) and DAPI (blue; A). Representative immunohistochemistry images demonstrating loss of glomerular capillary Ehd3 and increased Ehd4 expression in diabetic mice compared to control mice (B). Glomerular capillary Ehd3 protein expression was significantly decreased (C) and glomerular mRNA expression significantly decreased (D) in diabetic compared to control mice. Glomerular capillary Ehd4 (E) and glomerular mRNA (F) expression was significantly increased in diabetic compared to control mice. G, glomerulus; PC, peritubular capillary (A). Scale bars 25µm (A), 10µm (B); * P <0.05, ** P <0.01, *** P <0.001, *** P <0.0001.

Figure 6: GEnC fenestral changes are present in diabetic patients and are associated with eGFR and loss of glomerular EHD3 expression.

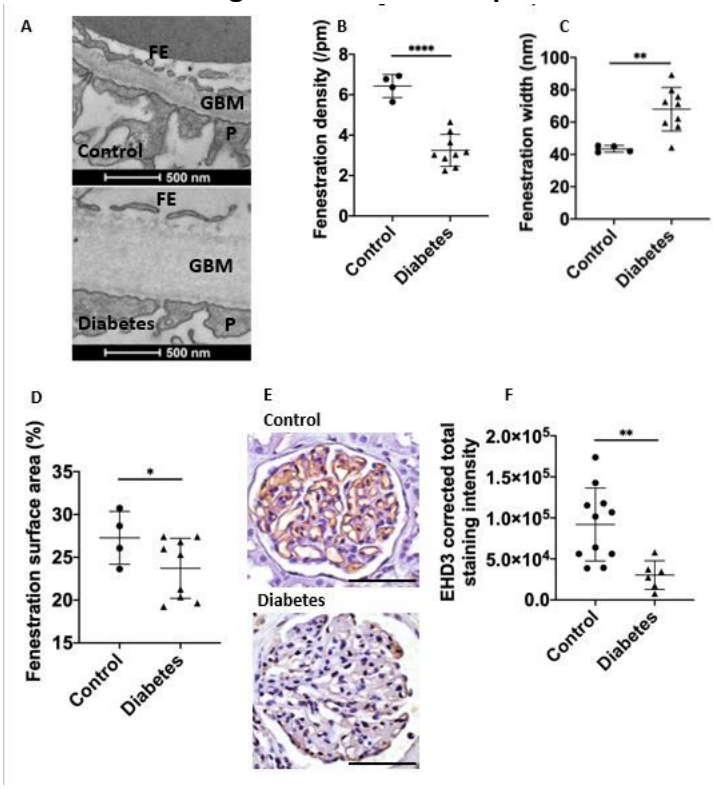

Representative transmission electron micrograph from human control and diabetic patients (A). GEnC fenestration density was significantly decreased (B), GEnC fenestration width significantly increased (C) and fenestration surface area significantly decreased (D) in human diabetic compared to control patients. Representative immunohistochemistry images demonstrating loss of glomerular capillary EHD3 (E) in diabetic compared to control human patients. Glomerular capillary EHD3 protein expression was significantly decreased (F) in diabetic compared to control human patients. Scale bar 100µm (D); * $P < 0.05$; ** $P < 0.01$; **** $P < 0.0001$.

Figure 7: Glomerular PLVAP expression is increased and EHD3 expression decreased in human diabetic patients.

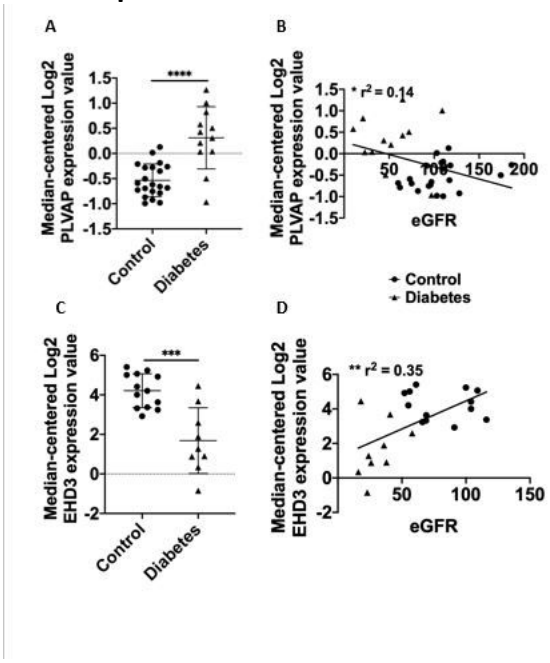

Data from Nephroseq (median-centered Log2 PLVAP expression) demonstrating increased PLVAP (A) in diabetic (n=12) compared to control healthy living donor patients (n=21) and a significant negative relationship with eGFR (B). Data from Nephroseq (median-centered Log2 EHD3 expression) demonstrating decreased EHD3 (C) in diabetic (n=9) compared to control healthy living donor patients (n=13) and a significant positive relationship with eGFR (D). Bold line indicates line of regression for all data points in (C, D); * P <0.05; ** P < 0.01; *** P < 0.001; **** P < 0.0001.

Figure 8: Ehd3 knockdown decreases fenestration formation in b.End5.

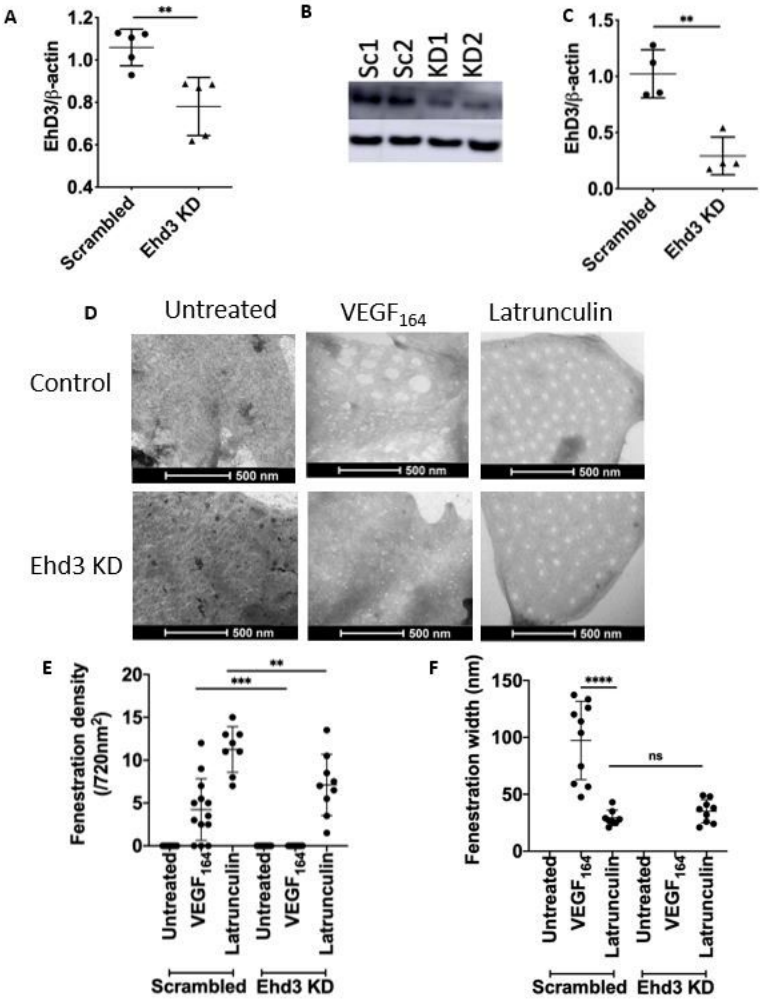

Ehd3 mRNA (A) and protein (B, C) knockdown was confirmed in a fenestration forming cell line (mouse brain endothelioma; b.End5). Western blot image confirming knockdown of Ehd3 in b.End5 (B). Representative whole mount TEM images of b.End5 control and Ehd3 knockdown cells demonstrating fenestration formation in response to $VEGF_{164}$ and Latrunculin A (D). Fenestration formation was significantly decreased in b.End5 Ehd3 knockdown cells compared to control cells in response to Latrunculin A treatment with complete absence of fenestration formation in response to $VEGF_{164}$ treatment (E). There was no significant difference in fenestration width in response to Latrunculin A treatment in b.End5 Ehd3 cells compared to control cells (F). Fenestrations formed in control cells in response to $VEGF_{164}$ were significantly wider than those formed in response to Latrunculin A treatment (F). KD, knockdown; Sc, scrambled; ns, not significant; ** $P < 0.01$; *** $P < 0.001$; **** $P < 0.0001$.

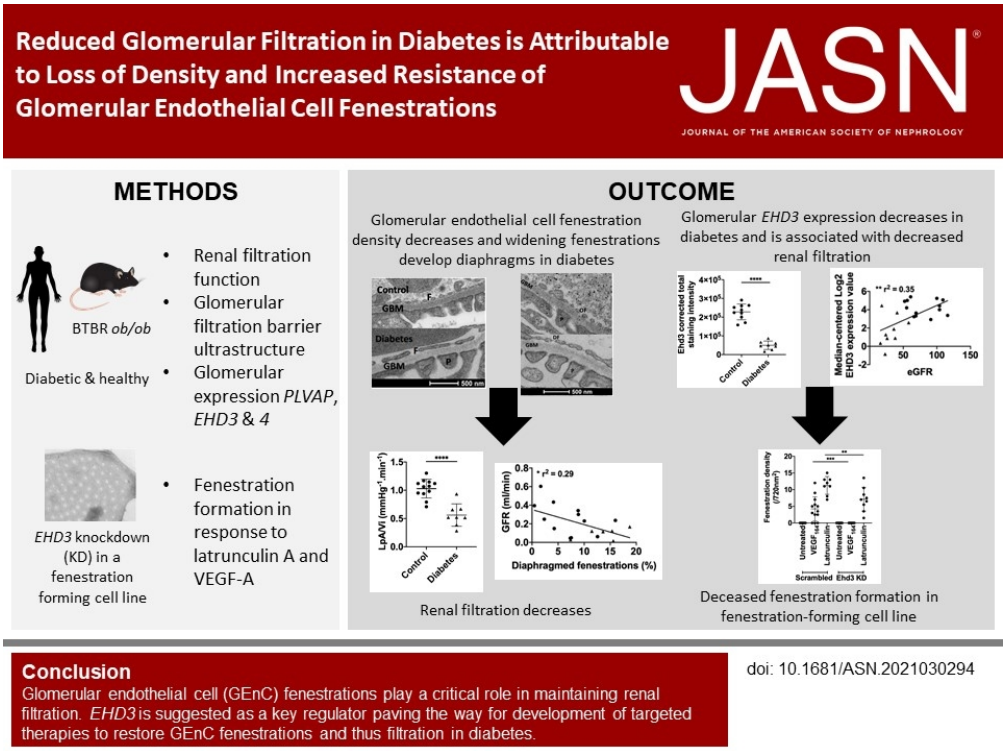

doi: 10.1681/ASN.2021030294

254x190mm (96 x 96 DPI)

Table of contents

Supplementary information S1: Total length of glomerular endothelium per image analysed. A total of 274 images were analysed from BTBR *ob*$^{-}$/*ob*$^{-}$ mice and 144 from BTBR *ob*$^{+}$/*ob*$^{+}$ diabetic mice. There was no significant difference in the length of endothelium analysed per image between control and diabetic mice. ns, not significant.

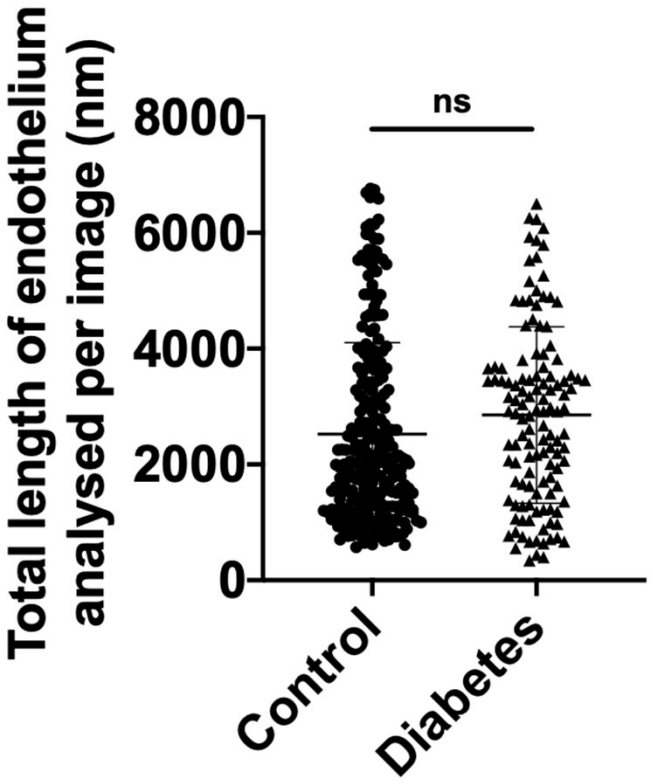

Supplementary information S2: Mathematical modelling to determine the contribution that the glomerular endothelium changes in diabetes make to the observed changes in functional properties of the glomerular capillary wall.

Mathematical modelling used the approach described by Drumond & Deen[6] based on a unit cell of the glomerular capillary wall

Fraction of the capillary surface occupied by fenestra (E_f) = $\{\pi.R_f^2*N_f\}/A$

where R_f = fenestral radius

where N_f = number of fenestra per unit cell

where A = cross-sectional area of the unit cell (*distance between slit diaphragms*)

Mean ultrastructural measurements obtained from BTBR *ob/ob* mice at 20 weeks:-

Fenestration density: control = 6.45, diabetes = 4.16

Fenestration width: control = 56.89 (radius = 28.45), diabetes = 75.03 (radius = 37.52)

Distance between slit diaphragms was not measured as part of the ultrastructural measurements. Therefore, as podocyte slit density significantly decreases and foot process width significantly increased, preliminary calculations were based on the assumption that A doubled in diabetes: i.e control A = 1, diabetes A = 2.

Control Ef = { π *28.45*28.45*6.45}/1 = 16401 units

Diabetes Ef = { π *37.5*37.5*4.25}/2 = 9199 units

In addition, the appearance of a diaphragm within fenestrae will further reduce the fractional surface area of each endothelial fenestra available for fluid filtration. In other capillary beds, this diaphragm-attributable reduction is in the order of 57% (Bearer & Orci, 1985, J Cell Biology). Taking measurements from Bearer & Orci (1985, J Cell Biology) average fenestra diameter ~188nm, average number of channels between radial fibrils of diaphragm = 15, average arc width of each inter-fibril channel = 5.46nm. Hence, 5.46*15)/188 = 0.43. Assuming a similar diaphragmatic ultrastructure, based on data in our study, there is an additional 6.62% of percentage of diaphragmed fenestra in diabetic capillaries (mean percentage diaphragmed fenestra in control = 7.04% and diabetes = 13.66%.) This results in a further reduction of Ef in diabetes to 8852 units based on:-

An additional 6.62% of diabetic fenestrae have a 0.43 individual Ef available for filtration

9199*6.62% = 609

9199 - 609 = 8590

609*0.43 =262

8590 + 262 = 8852 units

This reduction in Ef is in the order of 8852/16401 = 54% of control values

Supplementary information S3: Podocyte and glomerular basement membrane measurements confirming developing of diabetic nephropathy and glomerular volume in BTBR *ob*$^{-}$/*ob*$^{-}$ mice. In BTBR *ob*$^{+}$/*ob*$^{+}$ (n=8) diabetic compared to BTBR *ob*$^{-}$/*ob*$^{-}$ (n=13) litter mate control mice aged 20 weeks, podocyte slit density (A) was significantly decreased, podocyte foot process width (B) and glomerular basement membrane thickness (C) were significantly increased and there was no significant difference in podocyte slit width (D). Glomerular volume of individual glomeruli from BTBR *ob*$^{+}$/*ob*$^{+}$ diabetic mice was not significantly different from BTBR *ob*$^{-}$/*ob*$^{-}$ litter mate control mice (E). ns, not significant; * P <0.05; ** P <0.01; *** P <0.001.

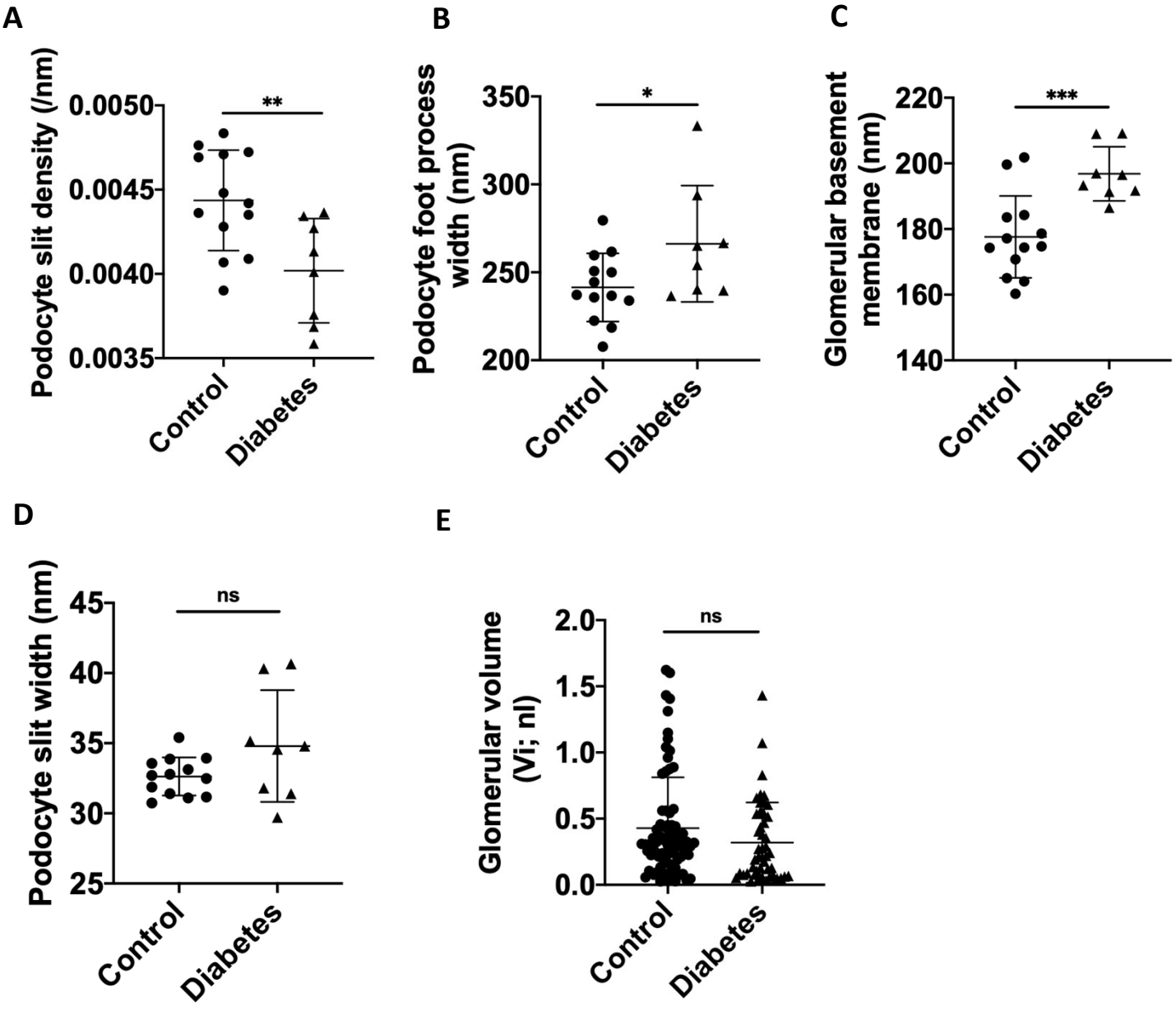

Supplementary information S4: Reduction in GEnC fenestration density and increase in width are associated with reduced glomerular ultrafiltration coefficient and GFR in BTBR *ob*$^{-}$/*ob*$^{-}$ mice. The relationship between GEnC fenestration density and glomerular ultrafiltration coefficient (A), GEnC fenestration density and GFR (B), GEnC fenestration width and glomerular ultrafiltration coefficient (C) and GEnC fenestration width and GFR (D) in diabetic and control mice aged 20 weeks. There was a significant positive relationship between GEnC fenestration density and glomerular ultrafiltration coefficient and GEnC fenestration density and GFR. There was a significant negative relationship between GEnC fenestration width and glomerular ultrafiltration coefficient and GEnC fenestration width and GFR. Bold line indicates line of regression for all data points. * $P < 0.05$; ** $P < 0.01$.

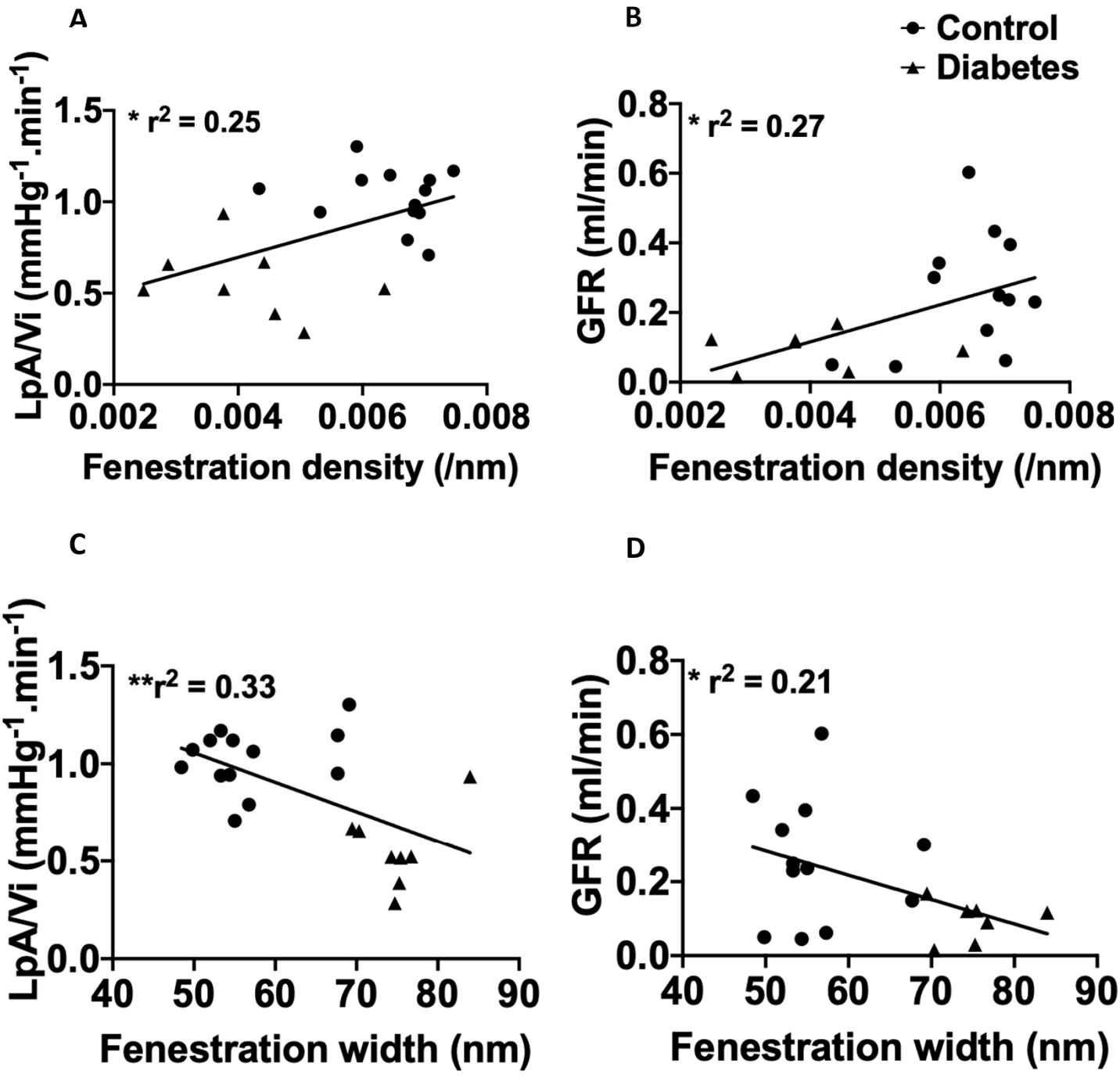

Supplementary information S5: Pearson's correlation between glomerular Ehd3 and Ehd4 expression and podocyte and GBM measurements. GBM, glomerular basement membrane; * P <0.05; ** P <0.01.

	Podocyte slit density	Podocyte slit width	Podocyte foot process width	GBM thickness
Ehd3	0.56*	-0.40	-0.39	-0.68**
Ehd4	-0.46	0.31	0.22	-0.68**

Supplementary information S6: Patient demographics, diagnosis and eGFR. Patient population for electron microscopy studies (A), patient population for immunohistochemistry studies (B). m, male; f, female; DM, diabetes mellitus; TMD, thin membrane disease; eGFR, estimated glomerular filtration rate

A

Patient	Age	Sex	Diagnosis	eGFR
1	55	m	Type 2 DM	47
2	49	f	Type 2 DM	40
3	53	m	Collagen 4 defect	70
4	25	f	Type 1 DM	77
5	78	m	TMD	55
6	61	m	Type 2 DM	84
7	51	f	Type 2 DM	38
8	45	m	Type 2 DM	25
9	52	m	Type 2 DM	43
10	30	f	TMD	88
11	25	f	Type 1 DM	30
12	34	f	TMD	117
13	42	m	Type 1 DM	24

B

Patient	Age	Sex	Diagnosis	eGFR
1	55	m	Type 2 DM	32
2	59	f	Type 2 DM	31
3	78	m	TMD	55
4	46	f	TMD	104
5	31	f	TMD	113
6	49	f	Type 1 DM	64
7G	31	f	Type 1 DM	32
8H	51	m	Type 2 DM	43
9I	13	f	TMD	111
10J	65	f	TMD	26
11	2	m	Transplant tissue	n/a
12	50	f	DM, Transplant tissue	n/a
13	51	m	Transplant tissue	n/a
14	70	m	Transplant tissue	n/a
15	55	m	Transplant tissue	n/a
16	70	f	Transplant tissue	n/a
17	n/a	n/a	Transplant tissue	n/a

Supplementary information S7: Podocyte and glomerular basement membrane measurements confirming developing of diabetic nephropathy in human diabetic patients. In diabetic (n=9) compared to control^{-} (n=13) human patients, podocyte slit density (A) was significantly decreased, podocyte slit width (B) and glomerular basement membrane thickness (C) were significantly increased and there was no significant difference in podocyte foot process width (D). ** P < 0.01; *** P < 0.001; **** P < 0.0001

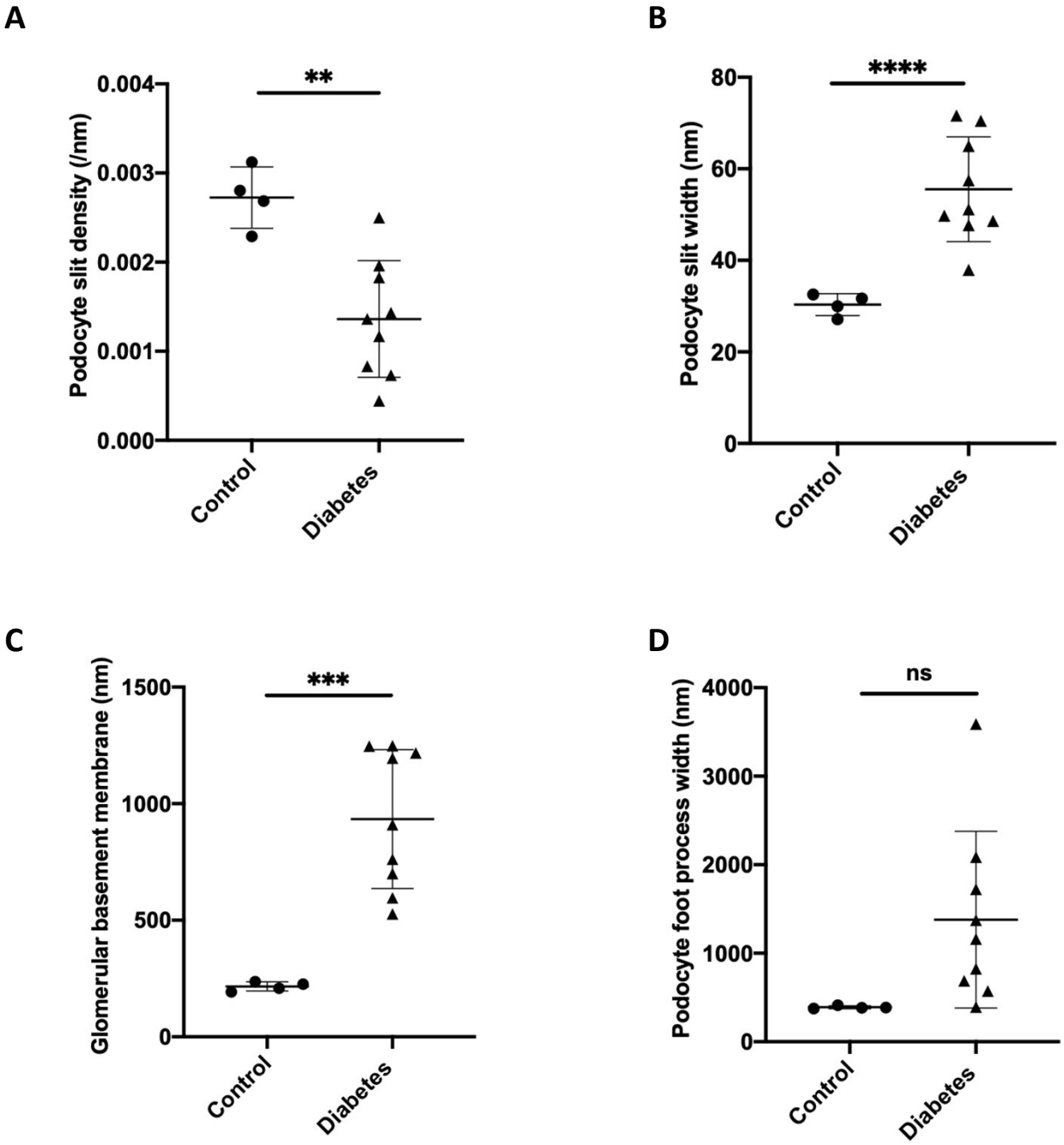

Supplementary information S8: Glomerular EHD4 expression is significantly increased in human diabetic patients compared to controls. Representative IHC image demonstrating increased glomerular EHD4 expression in diabetic compared to control patients (A). In diabetic (n=6) compared to control^{-} (n=11) human patients, glomerular EHD4 expression determined by IHC was significantly increased (B). Scale bars 100µm (A); *** P < 0.001